KADİR HAS UNIVERSITY
GRADUATE SCHOOL OF SCIENCE AND ENGINEERING
PROGRAM OF COMPUTATIONAL BIOLOGY AND BIOINFORMATICS

ENHANCED STRUCTURAL, OPTICAL AND ANTIBACTERIAL PROPERTIES OF ZnO DOPED TiO_2 COMPOSITES

MEHMET EYMEN SÜMER

Assoc. Prof. Dr. BENGÜ ÖZUĞUR UYSAL

MASTER'S THESIS

ISTANBUL, JUNE, 2021

ENHANCED STRUCTURAL, OPTICAL AND ANTIBACTERIAL PROPERTIES OF ZnO DOPED TiO_2 COMPOSITES

MEHMET EYMEN SÜMER
Assoc. Prof. Dr. BENGÜ ÖZUĞUR UYSAL

MASTER'S THESIS

Submitted to the Graduate School of Science and Engineering of
Kadir Has University in partial fulfillment of the requirements for the degree of
Master of Science in Program of Computational Biology and Bioinformatics

ISTANBUL, JUNE, 2021

DECLARATION OF RESEARCH ETHICS / METHODS OF DISSEMINATION

I, MEHMET EYMEN SÜMER, hereby declare that.

- this master's thesis is my own original work and that due references have been appropriately provided on all supporting literature and resources.
- this master's thesis contains no material that has been submitted or accepted for a degree or diploma in any other educational institution.
- I have followed "Kadir Has University Academic Ethics Principles" prepared in accordance with "The Council of Higher Education's Ethical Conduct Principles".

In addition, I understand that any false claim in respect of this work will result in disciplinary action in accordance with university regulations.

MEHMET EYMEN SÜMER
TARİH VE İMZA

ACCEPTANCE AND APPROVAL

This work entitled **ENHANCED OPTICAL, STRUCTURAL AND ANTIBACTERIAL PROPERTIES OF ZnO DOPED TiO_2 COMPOSITES** prepared by **Mehmet Eymen Sümer** has been judged to be successful at the defense exam held on 14.07.2021 and accepted by our jury as **MASTER'S THESIS.**

APPROVED BY:

Assoc. Prof. Dr. Bengü Özuğur Uysal (Advisor)	Kadir Has University	_____
Assoc. Prof. Dr. Gökhan Kirkil	Kadir Has University	_____
Asst. Prof. Dr. Hakan Kaygusuz	Altınbaş University	_____

I certify that the above signatures belong to the faculty members named above.

_____

(Unvanı, Adı ve Soyadı)

Dean of Graduate School of Science and Engineering

DATE OF APPROVAL: Gün/Ay/Yıl

TABLE OF CONTENTS

ENHANCED OPTICAL, STRUCTURAL AND ANTIBACTERIAL PROPERTIES OF ZnO DOPED TiO_2 COMPOSITES

ABSTRACT

In daily life, bacterial infections are common issues for human health. Thus, researchers are searching for valuable materials to prevent antibacterial infections and environmental pollutants. Thin film is a well-known application for photocatalytic and biological activity. Hence, thin-film formation is an excellent way to overcome these problems due to its nanosize thickness and enhanced monolayer or a multilayered structure. The most common material for the production of a thin film is titanium oxide (TiO_2). It has various traits to enhance the activity of thin films, such as structural and optical properties. However, single usage of pure TiO_2 has some limitations over these problems. Therefore, new techniques need to be implemented to overcome these limitations, and it is called doping. Doping is a standard method for manipulating material properties to provide enhanced functionality.

Thus, ZnO was selected as a dopant due to its good bandgap energy and high electron activity. Therefore, this thesis mainly focused on the antibacterial, structural, and optical activity differences of pure TiO_2 and ZnO doped TiO_2. Within several different thin film deposition methods, the sol-gel method was used in this research due to its easy progression at room temperature, low cost, and homogeneity traits. UV-vis spectrophotometer (Labomed Spectro 22) was used for optical analysis in the spectral range of 190–1100 nm wavelengths. Structural differences include homogeneity and particle size were determined by an X-ray diffractometer (XRD, Philips PW-1800). Antibacterial activity of pure and doped TiO_2 thin films was analyzed by the standard of ISO 22196 protocol against gram-positive “Staphylococcus aureus” and gram-negative “Escherichia coli”. As a result, XRD and UV-vis spectrophotometer measurements show that our dopant ZnO efficiently enhances the bandgap energy of pure TiO_2, and the correlation between dispersibility and homogeneity was achieved in the concentration range of ZTA-B-R (5-10).

Keywords: Thin film, TiO_2, ZnO, Doping, Sol-gel, XRD, UV-vis spectrophotometer, Antibacterial.

ZnO KATKILI TiO_2 KOMPOZİTLERİN GELİŞTİRİLMİŞ OPTİK, YAPISAL VE ANTİBAKTERİYEL ÖZELLİKLERİ

ÖZET

Günlük yaşamda bakteriyel enfeksiyonlar insan sağlığı için yaygın bir sorundur. Bu nedenle araştırmacılar, antibakteriyel enfeksiyonları ve çevresel kirleticileri önlemek için değerli materyaller arıyorlar. İnce film, fotokatalitik ve biyolojik aktivite için iyi bilinen bir uygulamadır. Bu nedenle, ince film oluşumu, nano boyutlu kalınlığı ve geliştirilmiş tek katmanlı veya çok katmanlı yapısı nedeniyle bu sorunların üstesinden gelmek için mükemmel bir yoldur. İnce film üretimi için en yaygın malzeme titanyum oksittir (TiO_2). Yapısal ve optik özellikler gibi ince filmlerin etkinliğini arttırmak için çeşitli özelliklere sahiptir. Bununla birlikte, saf TiO_2'nin tek kullanımı bu problemlerde bazı sınırlamalara sahiptir. Bu nedenle, bu sınırlamaların üstesinden gelmek için yeni tekniklerin uygulanması gerekir ve buna doping denir. Doping, gelişmiş işlevsellik sağlamak için malzeme özelliklerini manipüle etmek için standart bir yöntemdir.

Bu nedenle, iyi bant aralığı enerjisi ve yüksek elektron aktivitesi nedeniyle ZnO katkı maddesi olarak seçilmiştir. Böylece, bu tez temel olarak saf TiO_2 ve ZnO katkılı TiO_2'nin antibakteriyel, yapısal ve optik aktivite farklılıklarına odaklanmıştır. Diğer farklı ince film biriktirme yöntemleri içinde, oda sıcaklığında sürecin kolay ilerlemesi, düşük maliyeti ve homojenlik özellikleri nedeniyle bu araştırmada sol-jel yöntemi kullanılmıştır. UV-vis spektrofotometre (Labomed Spectro 22), 190–1100 nm dalga boyu spektral aralığında optik analiz için kullanılmıştır. Homojenliği ve parçacık boyutunu içeren yapısal farklılıklar, X-ışını difraktometresi (XRD, Philips PW-1800) tarafından belirlenmiştir. ISO 22196 protokolü standardına göre gram pozitif "Staphylococcus aureus" ve gram negatif "Escherichia coli"ye karşı saf ve katkılı TiO_2 ince filmlerin antibakteriyel aktivitesi analiz edilmiştir. Sonuç olarak, XRD ve UV-vis spektrofotometre ölçümleri, katkı maddesi ZnO'nun saf TiO_2'nin bant aralığı enerjisini verimli bir şekilde arttırdığını ve ZTA-B-R (5-10) konsantrasyonu aralığında dağılabilirlik ve homojenlik arasındaki korelasyonun sağlandığını göstermiştir.

Anahtar Sözcükler: İnce film, TiO_2, ZnO, Katkılama, Sol-jel, XRD, UV-vis spektrofotometre, Antibakteriyel.

ACKNOWLEDGEMENTS

I would like to thank my advisor (Assoc. Prof. Bengü Özuğur Uysal) for her guidance and support. I would also like to thank all my faculty members of the Computational Biology and Bioinformatics Department. Last but not least, I would like to thank my family, friends, and colleagues for their support and encouragement.

LIST OF TABLES

LIST OF FIGURES

LIST OF SYMBOLS/ABBREVIATIONS

α	Alpha
λ	Lambda- wavelength
θ	Theta-Bragg angle
A	Absorbance
cm	Centimeter
D	Diameter
ε	Extinction coefficient
K	Shape factor
μm	Micrometer
nm	Nanometer
ART	Anatase-rutile mix
BRT	Brookite-rutile mix
CVD	Chemical Vapor Deposition
DSSCs	Dye-sensitized solar cells

FWHM	Full width at half maximum
LS	Lignosulfonate
MB	Methylene blue
MG-62	Osteosarcoma
PGE	Power conversion efficiency
PL	Photoluminescence
Rb	Rose Benga
UC6	Human bladder tumor
UV	Ultraviolet
XRD	X-ray Diffraction
Ag	Silver
AgNO3	Silver nitrate
Au	Gold
Cd	Cadmium
Cu	Carbon
DI	Deionized water
GO	Graphene oxide
HCI	Hydrochloric acid
HNO3	Nitric acid
ITO	Indium tin oxide

NiO	Nickel oxide
Pt	Platin
Pd	Paladyum
SnO2	Tin oxide
TBOT	Tetrabutyl orthotitanate
TIP	Titanium isopropoxide
TiO_2	Titanium oxide
TTIP	Titanium tetra isopropoxide
ZnAc	Zinc acetates dehydrate
ZnO	Wurtzite
ZnO-TiO2	Zno doped TiO2
WO3	Tungsten oxide
eV	Electronvolt
meV	Million electronvolt
A.flavus	Aspergillus flavus
E. coli	Escherichia coli
S.aureus	Staphylococcus aureus
S.epidermidis	Staphylococcus epidermidis

1. INTRODUCTION

Material science and bioengineering are important majors of human life. Thus, a collaboration of these two different majors can be beneficial for biotechnological advancement. This thesis mainly focused on discovering valuable materials which can be used in biomedical applications or environmental remediation. Before starting the research, materials need to be determined and selected according to their different usage areas. In this research, primary materials need to be multifunctional. Therefore, the primary material is chosen according to its multifunctional capability in both biology and material science. Titanium oxide (TiO_2) is one of the best favorable materials for its unique traits. Titanium oxide (TiO_2) is also promising material due to its photocatalytic, semi-conductive, high degradation, easy to process, and low-cost traits (Luttrell et al., 2014). Titanium oxide (TiO_2) is commonly used for thin-film and coating applications. However, sometimes using single material can produce some problems because of materials' limitations, and often, these limitations are overcome by using dopants. A cross-section of these limitations needs to be handled correctly to get the desired result (Firdaus et al., 2012).

Therefore, the addition dopants need to be selected to synergize with titanium oxide and overcome its limitations. Every dopant has different bandgap energy, recombination rate, electron mobility, surface structure, and other features. Thus, dopants generally enhance the activity of primary material due to their beneficial effects on structural, morphological, chemical, and physical traits (Khlyustova et al., 2020). Therefore, dopants' addition may manipulate the TiO_2 main features such as surface area, recombination rate, bandgap energy level, optical and other traits (Khlyustova et al., 2020). For example, recent research shows that zinc oxide ZnO (wurtzite); has good electron activity at room temperature and has expansive bandgap energy compared to TiO_2 phases (Firdaus, Rizam, Rusop, & Hidayah, 2012). Therefore, ZnO-doped TiO_2 and three pure TiO_2 phases were used for the experimental process.

In this thesis, the sol-gel method primary method for the preparation of thin films. The sol-gel method creates highly efficient and homogenous thin films with low cost and less

time consumption. One of the main advantages of using the sol-gel method is to create homogenous material at room temperature. Homogeneity and sustainability are too essential for biomedical applications, and the sol-gel method can provide these traits by controlling the reaction's stoichiometry without creating unwanted residue (Pant et al., 2019). In characterization and determination of structural, optical and antibacterial traits of TiO_2 was achieved by several instruments such as UV-vis spectrophotometer, XRD and ISO 22196 protocol, respectively. UV-vis Spectrophotometer was provided absorbance values of different doped and undoped materials (Skoog, West, Holler, & Crouch, 2004). After this measurement, resonance ratio and normalize width calculation done for the homogeneity testing. Homogeneity and sustainability necessary for TiO_2 studies due to its applications areas include biomedical and environmental areas. Thus homogeneity determination process is achieved by tracking the correlation between resonance ratio and normalize width. These two measurements give thehomogenity and dispersibilty trait of materials (Tan & Resasco, 2005) . Bandgap energy manipulation is significant for the photocatalytic and antibacterial activity of TiO_2. Energy band gap correlation between doped and undoped composites was achieved by using the Tauc pilot. It demonstrates the direct and indirect conductivity levels of different composites TiO_2 is an indirect semiconductor, and ZnO is a direct conductor, and the combination of these two materials tends to go either indirect or direct (Firdaus et al., 2012). Determination of these conductivity levels was found using the Tauc intensity- wavelength graphs. XRD analysis shows the average particle size of doped and pure TiO_2 materials. The addition of new materials tends to create impurities, but using the sol-gel method prevents this problem and provides a good result for the brookite phase and a minor advancement for the anatase and rutile phase. However, the experimental result shows that our doping process provides a promising result for further implementation and hints at which concentration levels are critical for structural, optical, and antibacterial enhancement.

2. LITERATURE REVIEW

2.1 General Information about TiO_2

Titanium dioxide (TiO_2) is the second transition metal, and it is a valuable material for material science and biomedicine. William Gregor discovered TiO_2 in 1791, and Heinrich Klaproth isolates it. Titanium dioxide (TiO_2) has a bright white color, and it has three crystalline phases: anatase, brookite, and rutile (Zhang & Banfield, 2014). Titanium dioxide (TiO_2) is an excellent semiconductor in terms of bandgap energy, such as anatase 3.20 eV, rutile 3.00 eV, and brookite 3.13 eV (Linsebigler, Lu, & Yates, 1995; Thiyagarajan, Sivakumar, & Rajangam, 2016; Wang, He, Lai, & Fan, 2014). The anatase and brookite phases naturally transform into the rutile phase under high temperatures, and this trait makes the rutile phase the most stable phase (Zhang & Banfield, 2014). Its morphology highly depends on its phase differences and chemical manipulation, such as dopant addition. In addition, titanium dioxide (TiO_2) has multifunctional traits such as high recombination rate, biodegradability, and photocatalytic activity in higher temperatures (I M Joni, 2018). TiO_2 is used in various areas such as dye-sensitized solar cells, ion batteries, gas sensors, filters, light sensors, humidity sensors, hydrogen sensors, tissue engineering, biomedical and biodegradable treatments, industrial dyes, textile, and environmental remediation. (I M Joni, 2018).

2.2 TiO_2 Phases and Usage Areas

Anatase, brookite and rutile are the three main phases of TiO_2 (Luttrell et al., 2014). All these phases have distinct abilities and provide different advantages due to their different structural and chemical activity. For example, anatase has a tetragonal structure, and brookite has an orthorhombic structure (Zhang & Banfield, 2014). Moreover, the anatase phase is the initial phase formed in many applications, and then it transforms brookite and rutile in high temperatures, respectively.

Anatase has the largest bandgap than others phases and this trait making anatase more photocatalytic than the others (Luttrell et al., 2014). However, rutile can be more stable in higher temperatures, and it has the highest refractive index (Joni, 2018). Transformation of anatase to the rutile phase is irreversible. Brookite is rarely seen compared to anatase and rutile because its production is too hard for lab conditions.

However, brookite has the most significant cell volume, and that feature makes the brookite phase valuable for biomedical and environmental treatments (Zhang & Banfield, 2014) . Many studies show that mixed phases are more impactful than pure TiO_2 because of their limitations (Kumar et al., 2021). Literature reviews about TiO_2 phases and usage areas are a good starting point for understanding the advantages of different phases over different activities (Table 2.2.1).

Table 2.2.1. Industrial usage of TiO_2 according to its phase.

TiO_2 Phase	**Industrial Usage**	**References**
Rutile	Antibacterial agent	(Zainab, Olfat, & Faisal, 2019)
Rutile	Dye-sensitized solar cell	(Qureshi et al., 2021)
Rutile	Industrial dye	(Ojha & Thareja, 2020)
Rutile	Supercapacitors	(Su et al., 2021)
Rutile	Textile remediation	(Ambigadevi, Senthil Kumar, Vo, Hari Haran, & Srinivasa Raghavan, 2021)
Rutile	Tissue engineering	(Kolathupalayam Shanmugam et al., 2020)
Rutile	Degradation and loss of antibacterial activity	(Arce-Sarria, Machuca-Martínez, Bustillo-Lecompte, Hernández-Ramírez, & Colina-
Rutile	Sunscreen	(Yu et al., 2018)
Anatase	Antibacterial treatment	(Medvids et al., 2021)
Anatase	Oral multispecies Biofilm	(Pantaroto et al., 2018)
Anatase	Solar energy conversion	(Rajendhiran et al., 2021)
Anatase	Antibacterial activity of Ag-doped TiO_2	(Li et al., 2013)
Anatase	Humidity sensor	(Farzaneh, Mohammadzadeh, Esrafili, & Mermer, 2019)
Anatase	Wastewater treatment	(Ghouri, Elsaid, Abdala, Al-Meer, & Barakat, 2018)
Anatase	Acetone detection for diabetic patient	(Sabri et al., 2018)
Brookite	Photoluminescence enhancement	(Lamouchi, Slama, Saadallah, & Bouaicha, 2021)
Brookite	Photocatalytic and Photochemical	(Mutuma, Shao, Kim, & Kim, 2015)
Brookite	Environmental remediation	(Freire et al., 2021)
Brookite	Photocatalytic disinfection of bacteria	(Kumar et al., 2021)
Brookite	Shockwave resistance and energy storage	(Sivakumar et al., 2021)
Brookite	Biodegradation and wastewater treatment	(Lin et al., 2021).

The rutile TiO_2 phase is essential for various applications in biomedicine, dye-sensitized solar cells, industrial dye, supercapacitors, hydrogen sensors, textile, tissue engineering, dye-sensitized solar cells, supercapacitors, tissue engineering, hydrogen sensor, and sunscreen. Therefore, several experiments related to the rutile phases in literature were determined to benefit our research. In general, positive charges in liquid carried by metal oxide and negative charges are transported by a microorganism. This statement shows that metal oxide and microorganisms attract each other in liquid. Therefore, metal oxides are essential for treatment in antibacterial agents, and chemical attraction between these two can kill the microorganisms.

Furthermore, TiO_2's unique traits, such as its small size and high surface area, make them an excellent antibacterial agent (Zainab et al., 2019). In the dye-sensitized solar cell area, TiO_2 usage has been increased. Thus, regulating photoanode with doped TiO_2 can be so valuable due to its high surface area. As a result, doped TiO_2 based photoanode provides power conversion efficiency (PGE) due to increased charge transferability and bandgap energy level over other materials. This type of coordination can develop the solar cell industry without using harmful materials (Qureshi et al., 2021).

On the other hand, a combination of materials can increase the activity of the material. For example, graphene oxide (GO) is a promising remediation material because of its large surface area (2630 m^2/g). According to this trait, using graphene with TiO_2 may increase their photocatalytic activity. Furthermore, in reduced graphene oxide (GO) - TiO_2 showed good degradation traits compared to the single TiO_2. This information shows that doped TiO_2 can be more efficient than pure TiO_2 due to bandgap energy and recombination rate enhancement. This degradation enhancement was beneficial for industrial dye production (Ojha & Thareja, 2020).

Besides all the good traits of TiO_2, it has a relatively poor conductivity rate and low capacitative capability creates some problems. However, changing TiO_2 morphology can eliminate these minor problems and boost its capacitative capability. Doping TiO_2 with Nitrogen dopants shows this enhanced capacitative activity. The addition of Nitrogen(N) can overcome the limitation of TiO_2 and boost their capacitative rate by increasing the charge transportation of TiO_2 (Su et al., 2021). The textile industry is crucial for the world economy, producing textile dyes and pigments generally done by the chemical process.

However, their absorptive and reflective ability over sunlight creates environmental problems for some microorganisms.

Moreover, the end product of these materials is primarily carcinogenic and mutagenic. TiO_2 has a small spectrum range (400-700nm); hence, dopant addition is crucial for environmental treatments. For example, doping TiO_2 with non-metals can increase the required wavelength range of TiO_2 for photocatalytic activity on visible light by changing the bandgap energy level or recombination rate (Ambigadevi et al., 2021). Tissue engineering studies have arisen recently. Tissue engineering is vital for medical advancement because many people lose their tissues or organs due to medical or physical conditions. In this manner, some materials vital for the stability and longevity of products. In tissue engineering, biocompatibility and cytotoxicity are highly important. TiO_2 is known as good antibacterial material, and these traits make TiO_2 impactful on tissue engineering.

TiO_2 - based chitosan/sodium alginate nanocomposite was used in some experiments. Their test against human bladder tumor (UC6) and osteosarcoma (MG-62) cell lines result were promising. Their antibacterial traits were tested on Escherichia coli, and staphylococcus aureus also provides a good result. Both studies show that the chemical and physical attribution of TiO_2 based nanocomposite provides good biocompatibility, which means TiO_2 -based nanocomposite can be suitable for tissue engineering processes (Kolathupalayam Shanmugam et al., 2020). Breakdown of antibiotics and other drug waste is vital for environmental pollution. According to this problem, the breakdown of some commercial drugs needs to be studied. For example, the breakdown of amoxicillin is important for the drug industry. TiO_2 with tungsten oxide (WO_3) was studied and provided good results on the degradation of drug waste due to the photocatalytic activity of the TiO_2 composite.

TiO_2 with tungsten oxide (WO_3) inhibits the amoxicillin end product and other impurities. However, TiO_2 with tungsten oxide (WO_3) underperformed over commercial TiO_2, but it still decreases the number of byproducts from the drug. This result shows the importance of doped- TiO_2 material over drug activity and wastewater degradation.

Bioproducts such as sunscreens are also an essential topic for biomedical science due to their effect on the human body. TiO_2 with natural sun blocker-lignosulfonate (LS) - can enhance the photocatalytic activity of TiO_2. After the chemical alteration of two materials,

self-doping of hydroxylated TiO_2 and lignosulfonate (LS) oxidation increases the UV protection. This result shows that TiO_2 @LS composite can be used on sunscreen to prevent the harmful effect of UV light (Yu et al., 2018).

The anatase TiO_2 phase is essential for various applications in the antibacterial treatment, photocatalytic reactor, humidity sensor, wastewater treatment, a gas sensor for acetone detection, dye-sensitized solar cell, lithium-ion anodes, H_2S gas sensor. Several experiments related to the anatase phases in literature were determined for the benefit of our research. In recent studies show that using laser irradiation can enhance the activity of TiO_2 and its antibacterial activity. Besides UV activation, laser irradiation can provide new paths for TiO_2 activity. Furthermore, the thickness of the TiO_2 films can be manipulated with different laser irradiation, and this morphological advancement changes TiO_2 activity.

However, increasing heat creates mixed phases due to TiO_2 morphology-shifting anatase phase to rutile phase- and tends to affect homogeneity. Moreover, irradiation triggers antibacterial growth inhibition due to the increased photocatalytic activity of TiO_2. Therefore, laser irradiation can be appropriately applied for future studies to enhance the antibacterial activity of TiO_2 (Medvids et al., 2021). In another biomedical usage of TiO_2 is oral biofilm applications as a coating material. Different phases of TiO_2 -control, anatases, rutile, and anatase-rutile-were tested against three different species: Streptococcus sanguinis, actinomyces naeslundii, and fusobacterium nucleatum. As a result, a single anatase and anatase-rutile mixture can reduce bacterial activity and can be used on oral biofilms (Pantaroto et al., 2018). Thus, the plant leaf extract is used in medicine and other biomedical application. However, some studies suggest that the usage of plant extract with TiO_2 also enhances the photocatalytic activity of the material. For example, Plectranthus amboinicus leaf extract is used to synthesize TiO_2 nanoparticles.

The extracted TiO_2 nanoparticle treated with Indium tin oxide (ITO) and Rose Bengal (RB) dye to create dye-sensitized solar cells (DSSCs). Besides average DSSCs environmental pollution, TiO_2-based DSSCs can be more beneficial for the environment due to the power conversion and antibacterial activity of TiO_2. These TiO_2 based materials convert solar energy into electrical energy. Conversion of energies provides an excellent approach for wastewater treatment and reducing the waste product of non- TiO_2 DSSCs (Rajendhiran et al., 2021). Doping TiO_2 with other metals can be beneficial for

various applications. In this case, TiO_2 was doped with a silver (Ag) for antibacterial activity examination. Silver (Ag) is known as a good dopant material and is used in various applications. However, doping TiO_2 with a silver (Ag) and track their activity is crucial for clinic applications and material science. In addition, some studies show that Ag-doped TiO_2 can provide %100 antibacterial inhibition against Escherichia coli. Therefore, the synergetic reaction of Ag-doped TiO_2 is an excellent antibacterial material for biomedical applications (Li et al., 2013). Humidity sensors are crucial for human life. Producing humidity sensors relied on Cu-doped TiO_2 based nanocomposites can be enhanced the activity and balance of the sensor. Cu-doped nanocomposites show great promise for humidity sensors because Copper (Cu) can reduce the band gap value of TiO_2, thus increase the water molecule detection. The addition of a dopant can change the electrical traits of TiO_2 and increase its sensitivity. Most of the time, dopants increase the bandgap energy of TiO_2 but in some studies, reduction of band gap also beneficial for some applications (Farzaneh et al., 2019).

The mixed nanocomposite has various beneficial traits over wastewater treatment due to photocatalytic activity. One of them is hybrid nanostructured graphene-Pt/ TiO_2 studies. This hybrid nanocomposite can a breakdown of methylene blue (MB) dye under sunlight. Dopants on the high surface area enhance visible light interaction and increase the separation and transportation of electron/ hole pairs. In addition, Pt/ TiO_2 nanostructure provides excellent stability for the breakdown and removal of methylene blue (MB).

As a result, hybrid nanocomposites can be helpful on various treatment and still needs to examine with a different dopant concentration and fixation (Ghouri et al., 2018).

In human life, diabetes is a highly abundant disease. In some studies show that TiO_2 can be helpful to sense the gas presence. In biomedical treatment, TiO_2 may be used to detection of acetone. In one study, candle soot used as a dopant and enhance the activity range of TiO_2 to create an acetone sensing detector. A combination of soot and TiO_2 can highly photoactive and detect low UV intensities. These nanocomposites can be used as a sensitive layer to sense acetone presence by tracking the UV intensities. As a result, this sensitive layer can detect the acetone presence in humans and show their diabetes (Sabri et al., 2018).

The TiO_2 brookite phase is rarely seen in lab conditions due to its production process more complex than other phases, and most of the time, it is used with a combination of other phases—several experiments related to the brookite phases in literature determined for the health of our research. For the brookite phase, photoluminescence enhancement, photocatalytic disinfection of bacteria, shockwave resistance and energy storage, environmental remediation, biodegradation, and wastewater treatment was determined.

In the photoluminescence study, Nickel (Ni) and carbon (C) were used as doping materials for photoluminescence enhancement. Photoluminescence (PL) of engineered TiO_2 is a promising technology for optoelectronic device improvement.

In general, tuned doping materials improve photocatalytic efficiency, but suitable materials need to be found with several experiments to achieve good results. Ni and carbon are the best suitable material the enhanced photoluminescence enhancement. Doping with Ni decreased the surface resonance. The formation of the brookite phase enhances the crystallization of the layer at low temperatures. Transformation of TiO_2 from crystalline brookite to an amorphous state using low temperatures can boost PL activity (Lamouchi et al., 2021).

It is so important to distinguish the photocatalytic activity rate of different types of crystalline phases. Mixing phases is a suitable determination method for photocatalytic activity, such as anatase-brookite, anatase-brookite-rutile, and anatase-rutile.

For example, TiO_2 phases have different band gaps, such as anatase 3.20 eV, rutile 3.00 eV, and brookite 3.13 eV, respectively (Linsebigler et al., 1995; Thiyagarajan et al., 2016; Wang et al., 2014).

Due to their different bandgaps, their photocatalytic activity is different from each other. Recent studies have shown that the brookite phase is also a suitable photocatalyst due to its orthorhombic structure(less symmetrical) and high bandgap range like anatase. Therefore, using a mixture of anatase-brookite may be increased the recombination rate of pure anatase or rutile. Furthermore, using an anatase-brookite mixture and testing their efficiency over pure anatase or rutile also suitable for chemical and physical stability and homogeneity studies. Hence, changing environmental conditions such as pH and temperature can trigger the conversion of ART (anatase-rutile) or BRT(brookite-rutile) phases. Due to chemical and structural manipulation, traits of TiO_2 such as photocatalytic, biochemical, and antibacterial traits can be quickly shift desired way (Mutuma et al.,

2015). In environmental remediation studies, wastewater treatment by using TiO_2 brookite can provide a beneficial outcome. Many industrial companies and human activities consumed the water. Misusage of water consumption worldwide rapidly increases, and most of the company and scientist wants to discover the technique that can lead people to treat wastewater securely. Wastewater treatment can be possible by the usage of TiO_2. Exposing TiO_2 onto the wastewater removes the impurities by photocatalytic oxidation and photocatalysis. In the photocatalysis process, excited atoms change their band and create an electron-hole pair. TiO_2 initiates the oxidizing reaction on the compound surface due to its photocatalytic activation, and this process triggers the removal of organic pollutants and impurities by oxidation. Due to solid oxidizing abilities, low cost, and chemical stability, TiO_2 films are used as water filters. The production method is also essential to maintain TiO_2 film's lifetime and cost management. Several methods recognized as a suitable production method for TiO_2, such as chemical and physical deposition methods, are well-known production methods for TiO_2 films. Moreover, in some conditions, the anatase-brookite mixture tends to provide more photocatalytic activity than single anatase (Freire et al., 2021).

In general, water treatment is done by chlorine and chlorine-based chemicals, but these materials too expensive and include dangerous components for human health such as carcinoma and mutations. Furthermore, due to some limitations of TiO_2, usage of dopants increase rapidly.

Thus, TiO_2 is doped with several different materials to achieve a higher absorbance rate in recent years, such as Cd, NiO, and graphene-porphyrin. For example, in photocatalytic disinfection of bacteria studies, a porphyrin-doped TiO_2 - was used to examine the biochemical blockage examination of TiO_2. A porphyrin dopant was designed to increase the absorption rate of TiO_2 in visible light without affecting human life. Pure anatase and the brookite-rutile mixture were prepared for comparison. In addition, the photocatalytic disinfection ability was tested on gram-negative bacteria Escherichia coli (E. coli) in visible light. In general, gram-negative and gram-positive bacteria are common microorganisms to test, but especially gram-negative bacteria too important for TiO_2 experiments due to their cell wall. The cell wall of gram-negative bacteria contains a thin peptidoglycan layer covered with impermeable double layers containing some lipids and polysaccharides.

Due to its polysaccharide part, the negative charges permit the entrance of positively charged material. This interaction allows the materials to pass inside the cells and cause cell death. Due to this trait, hybrid TiO_2 materials may be used to treat wastewater as a coating material. (Kumar et al., 2021). Phase stability of TiO_2 is so crucial for a variety of applications such as solar systems, thermal protecting systems, aerospace applications, radiation absorption, medical application and solar energy conversion. Due to high demand on this topic, scientists explore new information about which TiO_2 crystalline structure more stable than the others in shockwave pressure circumstances. Recent studies suggest that brookite TiO_2 is more stable under 300 shocks, and anatase TiO_2 tends to transform into a rutile structure under that type of pressure. This information is vital in dealing with high-pressure environments and other critical assessments such as solar energy conversion and radiation absorption. Furthermore, due to its shock-absorbing trait, the brookite phase can be helpful for the harmful environment such as high pressured surfaces, energy conversion applications, biofilm coating (Sivakumar et al., 2021).

In the biodegradation studies, photocatalytic activity differences between pure phases and a mixture of TiO_2 phases are too significant. Fighting against bacteria is a crucial topic for health science, and one of the vital antibiotics in this area is fluoroquinolone (levofloxacin). Fluoroquinolone is used against a variety of harmful microorganisms such as bacteria and pathogens.

However, levofloxacin is not fully degradable in the human body after initial exposure, and the end product is spread into the environment. Due to this problem, levofloxacin degradation is vital for environmental remediation. In addition, adding doping materials on TiO_2 may create side impurities to act as a charge carrier and reduce the overall photocatalysis level of TiO_2 besides other advantages. Due to these problems, some studies suggest using a pure form of TiO_2 and looking at their efficiency against microorganisms.

In theory, a pure TiO_2 not enough to maintain the total photocatalytic activity of degradation. Therefore, a combination of the different TiO_2 phases was used for optimum efficiency. However, the pure brookite TiO_2 effectively fights against the biodegradation of levofloxacin and its wastewater treatment (Lin et al., 2021).

2.3 Determination and Discrimination of Experimental Method

In the production of TiO_2, various methods can be helpful, but the most important thing is time and money consumption. Recently, most of the technological advancement done by the nano-thickness scale and these types of materials provide various abilities in the biomedical, electrical, physical, chemical area. These new properties can be beneficial for bioactivity. The introduction of thin films on bioactivity can be beneficial for various applications. A single or multilayers create these films, and their thickness is changing from nanometers to few micrometers. These thin films contain two parts: the substrate and the layer part. These thin films provide various functions to execute against microorganisms, such as material transformation on wastewater's harmful environment or biodegradation. Due to these unique functionalities, the preparation of thin-film is too crucial for the outcome. Two different deposition techniques are viable in thin-film production, such as physical and chemical depositions (Table 2.3.1).

Table 2.3.1. Deposition methods

Chemical Deposition Techniques	Physical Deposition Techniques
1.Chemical Vapor Deposition (CVD)	**1.Sputtering techniques**
Low pressure (LPCVD)	Direct current sputtering (DC sputtering)
Plasma enhanced (PECVD)	Radio frequency sputtering (RF sputtering)
Atomic layer deposition (ALD)	**2. Evaporation Techniques**
2. Plating	Vacuum thermal
Electroplating technique	Electron beam
Electroless deposition	Arc evaporation
3.Chemical bath deposition	Molecule Beam epitaxy
4.Sol-gel technique	Ion Plating
5.Spray pyrolysis technique	Laser Beam
6.Hydrothermal synthesis	**3.Ball milling**
7.Spray coating	

All these deposition methods have unique ways to produce TiO_2 thin films, but determination and discrimination of most valuable methods are done according to cost, time-consuming, stability, and homogeneity. In between these two main deposition methods, our experiment more suitable for the chemical deposition method. Therefore, all standard deposition methods are listed and due to our limitation of budget and time interval analysis, choosing the sol-gel method is more beneficial for the experimental process (Table 2.3.2).

Table 2.3.2. Chemical deposition methods for TiO_2 thin film and their advantages as well as limitations

Method	Description	Advantages	Limitations	Ref.
Chemical Vapor Deposition (CVD)	A chemical reaction between the substrate and volatile precursors	-Easy method -Less contamination -Flexible -High density	- Toxic and flammable -Needs higher reaction temperature - Low deposition rate -More than one material creates chaos	(Yemmireddy & Hung, 2017) (Patil, Shaikh, & Ibram, 2015)
Sol-gel technique	Derived from precursor metal alkoxide using hydrolysis and condensation reaction	-Rate of reaction can be easily controlled -Homogeneity -Low cost -Reproducible - Deposition of several precursors	-High temperature -Problematic to attach a thick layer of nanoparticles on the substrate	(Varshney et al., 2016) (Yemmireddy & Hung, 2017) (Patil et al., 2015)
Spray pyrolysis	Precursor solutions become tiny droplets and then decompose by heated environment	-Easy and low cost - Complex structures can be coated -Easy to fabricate multilayer	-Oxidation of sulfides -Problem on determining growth temperature	(Varshney et al., 2016) (Mardare, Iacomi, Cornei, Girtan, & Luca, 2010)
Hydrothermal synthesis	Production of crystals from either single form or heterogeneous form reactions in aqueous soliton with high temperature and pressure.	-Simple -Capable of growing large -High-quality crystals	-Costly -Growth of crystal cannot traceable	(Varshney et al., 2016) (Patil et al., 2015)
Spray coating	Evaporating the solvent while spraying	-Easy to process -Low-cost -Scalable	-No homogeneity	(Deák et al., 2016) (Mérai et al., 2018)

2.4 Sol-Gel Method

The sol-gel method is a beneficial deposition technique to obtain a thin film for several different usage areas such as biomedical, chemical and electrical (Varshney et al., 2016). The sol-gel method was chosen for this experiment because of its unique traits such as homogeneity, sustainability, effectiveness, and low cost (Pant, Park, & Park, 2019). Homogeneity is crucial for this experiment because this experiment mainly focused comparison of ZnO doped TiO_2 thin films with pure TiO_2 thin films. Furthermore, the most significant advantages of using the sol-gel method are; it is carried out at room temperature and enhance various functions at a low cost (Pant, Park, & Park, 2019).

In general, the sol-gel method is a method of gel production derived from precursor metal alkoxides by using hydrolysis and condensation reactions (Jilani, Abdel-wahab, & Hammad, 2017). The primary sol-gel method has four steps: sol production, hydrolysis, condensation, drying (gel formation) (Aguilar, 2018) (Figure 2.4.1).

The starting materials generally chose from inorganic metal salt or metal alkoxides (Jilani et al., 2017). The sol-gel method offers the transition of solution (sol) into a solid (gel) phase. The "Sol" phase initially started with the dispersion of metal alkoxides or inorganic salt. After producing the "sol" phase, a solvent in the solution begins to evaporate, the left particles or ions begin to join and create a continuous network.

This continuous network creates a web structure, and this newly formed structure is called "gel." (Figure 2.4.1). However, acid and base addition can form a more dense or strict network (Aguilar, 2018). Transition to van der Walls bond interaction to covalent bond makes this process irreversible (C. Brinker, 1990). The main advantage of the sol-gel method is dissolving the precursor material in liquid with controlled stoichiometry. The rate of reaction can be easily controlled by temperature. This controlled stoichiometry prevents contamination and provides a suitable environment for mixing multi-compounds in the same solution. Shape, viscosity, porosity and texture can be controlled by changing dynamics of the sol-gel method (Dulian et al., 2019).

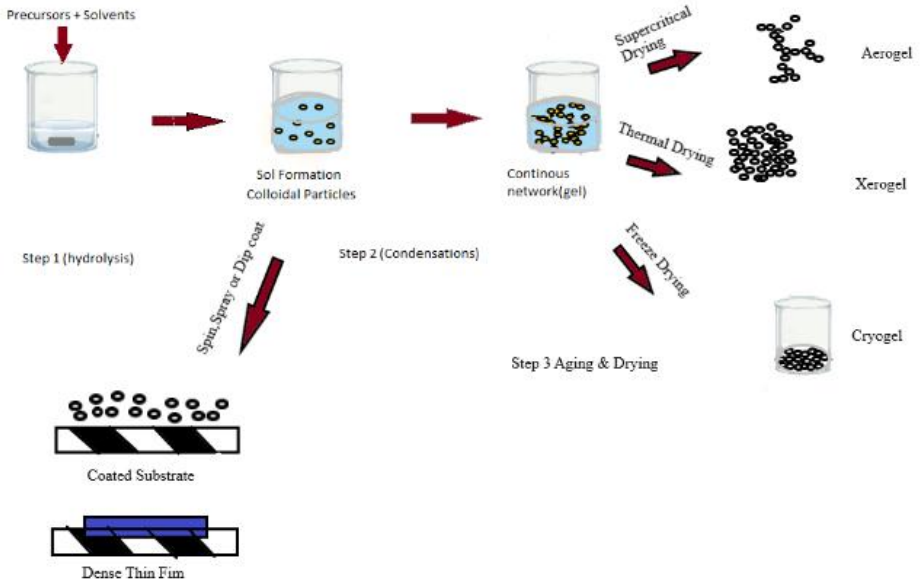

Figure 2.4.1. Stages of the sol-gel technique

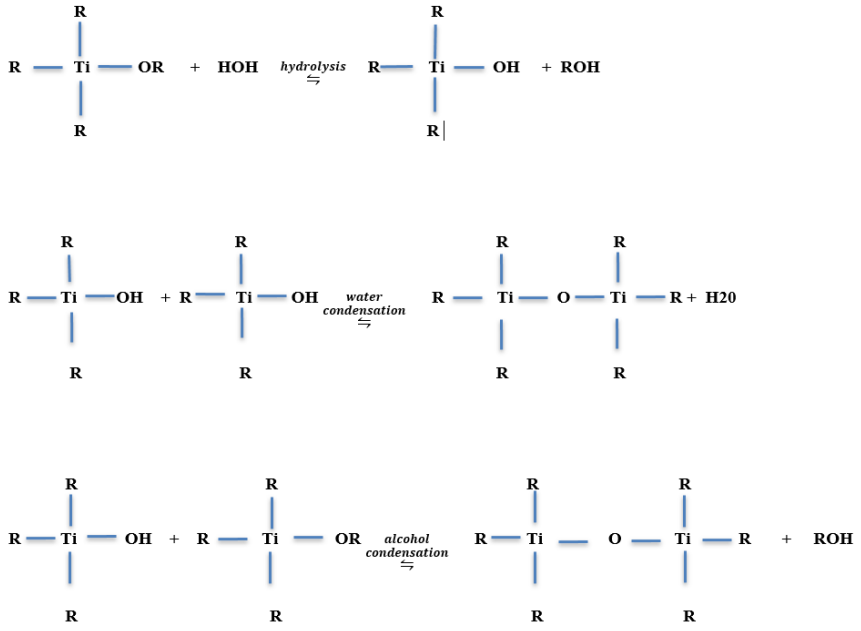

Figure 2.4.2. Reactions of sol-gel method

2.5 Doping Material

Doping is a commonly used method that provides various electrons and holes in semiconductors. In general, doping is known to modify conductivity by adding new materials into a semiconductor crystal. For example, doping of TiO_2 with various dopants forms new energy levels, and that process increases TiO_2 photocatalytic activity. However, doping material divides into two types: N and P-type doping. N-type doping is created between the material with a 4-valence electron semiconductor and a 5-valence electron dopant material—P-type material created between the material with 4-valence electron semiconductor and 3-valence electron dope material ((Khlyustova et al., 2020). N-type dopant increases the number of available electrons because dopant has one more valence electron than semiconductor (Table 2.5.1).

On the other hand, P-type dopant increases the number of holes because dopant has only three valance electrons that are less than semiconductor, and both these processes increase the conductivity of the semiconductor by changing bandgap energy differently. In general, the bandgap represents the minimum energy level for one electron, the jump next energy level where it can join in conduction (Khlyustova et al., 2020). Thus, a bandgap is a distance between the valence band and the conduction band (Figure 2.5).

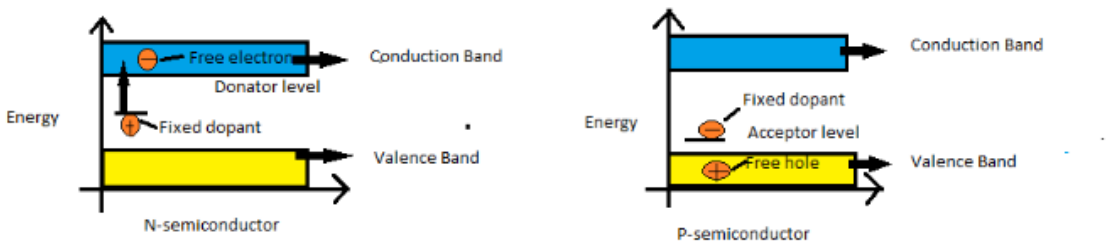

Figure 2.5. Representation of N-type and P-type of semiconductor

Table 2.5.1. Doping Material features

	N-type	P-type
Bonds	Extra Electron	Less Electron
Dopant	5-valent electron	3-valent electron
Carriers	Electrons	Hole

Many researchers have been studied various dopants for TiO_2 thin film experiments. Those dopants enhance the thin film photocatalytic and antibacterial activity in various ways (Norton et al., 2004). ZnO was chosen for this experiment because it has good electron mobility at room temperature and has an expansive bandgap energy of 3.37 eV compared to TiO_2 phases (Firdaus, Rizam, Rusop, & Hidayah, 2012). TiO_2 and ZnO are known as excellent semiconductors. However, their characteristics are different such as TiO_2 is an indirect semiconductor meanwhile ZnO is a direct semiconductor.

However, TiO_2 thin films present two limitations during photocatalytic activities: low use of solar spectrum and high recombination rate (Firdaus et al., 2012). ZnO is a good candidate for compensating for these limitations due to its unique traits. Recently, many researchers took advantage of nanocomposite materials due to their enhancing traits on optical, electrical and structural properties (Table 2.5.3) (Firdaus et al., 2012). Furthermore, dopants can increase the electron transfer efficiency of semiconductors. Hence, using noble metal ions, such as Au, Ag, Pt and Pd as a dopant can enhance the photocatalytic efficiency in various ways; catching electrons and reduce the recombination rate, and empower the light absorption in the visible range (Bensouici et al., 2015).

Overall, the addition of dopants can manipulate photocatalytic, chemical, and antimicrobial activity. However, combining new materials as a dopant still needs to improve because every different concentration of dopants can provide new outcomes.

Table 2.5.2. Specific features and values of ZnO material

Features	Value
Density	5.6006 g/cm^3
Melting Point	1975 ^{0}C
Energy gap	3.36 eV
Binding energy	60 meV

2.6 UV-vis Spectroscopic Method

Ultraviolet-visible (UV-vis) spectrophotometer is an absorbance determination material used to understand materials' optical features in solution or solid phase. This device tracks the excited atoms by looking at their wavelength and absorbance energies. UV-vis spectrophotometer detects the absorbance of the film between the range of 200-1100 nm spectrum (Skoog, West, Holler, & Crouch, 2004). The absorbance value is calculated by Beer-Lambert law (Equation 2.6.1).

For the single wavelength, A is absorbance (unitless), ε is known as an molar absorptivity (molar, $M^{-1}cm^{-1}$), b is the length of the path (cm), c is solution concentration (M), I_0 is the intensity of light at a specific wavelength, and I is the transmitted intensity (Skoog et al., 2004). Moreover, UV-vis spectroscopy can provide quantitative and qualitative information about of sample (Skoog et al., 2004).

$$\mathbf{A = \log_{10}(I_0/I) = \varepsilon bc,} \qquad \mathbf{(2.6.1)}$$

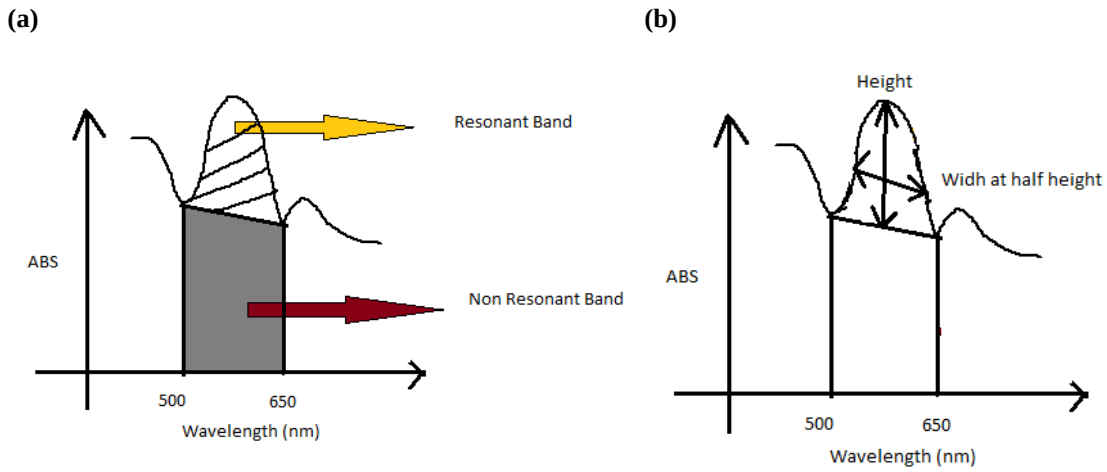

Figure 2.6.1. (a) Representation of resonant and non-resonant band **(b)** Representation of Height and Width at half height (FWHM)

In UV-vis spectrophotometric analysis' most crucial part is finding the area under the curve because the area under the curves gives the resonance ratio. The resonance ratio is an essential concept for homogeneity, and it has been calculated by dividing the resonant band area into a non-resonant band area. In addition, another critical concept called normalized width is calculated by the division of width of the resonant band into the height of the resonant band-both resonance ratio and normalized width important for optical analysis of materials (Tan & Resasco, 2005).

Resonance ratio = Area of resonant band/ area of the nonresonant band (2.6.2)

Normalized width= Width of resonance band/ height of the resonant band (2.6.3)

2.7 XRD Analysis

XRD is a widely used analytic method for physical and chemical composition identification. XRD instruments include three elements: a sample holder, an X-ray detector, and an X-ray tube. Generally, cathode tubes create the X-ray and voltage applied for accelerating the electrons than electrons bombarding the target material. Therefore, the XRD helpful method for analyzing homogeneity, crystal property, and average particle size. In general, XRD creates monochromatic X-rays, and these X-rays are scattered at specific angles to create specific peaks according to a sample's crystalline structure (Brady & Boardman, 1995).

Every material has a unique set of d-spacing which means converting diffraction peaks to d-spacing reveals the type of the material. Due to these traits, the XRD pattern reveals the atomic composition of the material. Moreover, XRD analysis provides the atomic position of the crystalline structure. XRD analysis application on thin films provides information about lattice formation between substrate and film, homogeneity of materials, quality of the film, thickness, and toughness of the thin film (Jeans, 1998). The XRD result shows the average crystal size using Scherrer's equation (Equation 2.7). In Equation 2.7, D represents the diameter of the TiO_2 nanocrystals, K presents the shape factor, and it has a constant value (0.89), λ represents the radiation wavelength, B represents the full width at half maximum (FWHM) of the diffraction line, and θ (theta) represents the Bragg angle (rad) (Valerio & Morelhão, 2019).

$$\mathbf{D} = \frac{K\lambda}{B\cos\theta}, \qquad \textbf{(2.7)}$$

2.8 Antibacterial Measurement

The antibacterial activity of TiO_2 is crucial for biodegradation, wastewater remediation and antibacterial disinfection. TiO_2 thin films used various applications related to antibacterial activity, and most of them are mentioned (Section 2.2). The advantages of TiO2 are photocatalytic activity, high degradation efficiency and non-toxicity (Phuinthiang et al., 2021). Due to these traits, TiO_2 thin film can provide a suitable solution for antibacterial disinfection studies.

Antibacterial materials rapidly grow in recent years, and most technological advancements need to provide antibacterial traits. Therefore, the ISO 22196 method was used to determine the antibacterial activity of TiO_2 thin films. In addition, ISO 22196 is a method that quantitatively evaluates the antibacterial activity (growth inhibition or killing) of samples such as plastic, other non-porous, and surface products (ICS, 2011). Therefore, ISO 22196 is an excellent method to determined bacteriostatic (growth inhibition) and bactericidal (killing bacteria) features and this test highly critical for TiO_2 usages for future technologies.

Different types of pure and doped TiO_2 thin film antibacterial efficiencies were represented (Table 2.8).

Table 2.8. Antibacterial efficiency of different types of Pure TiO_2 and doped TiO_2

Thin Film type	Bacteria type	Light Source	Highest Antibacterial inhibition %	References
Sn^{+4} - TiO_2 film	*E. coli, S.aureus*	UV	99.9%	(Sayılkan et al., 2009)
TiO_2 film	*S.aureus, S.epidermidis, E.coli*	UV	47 %	(Pleskova et al., 2011)
TiO_2 /Ag/Cu	*E. coli*	UV	100%	(Gospodonova, Ivanova, & Vladkova, 2021)
Mg- TiO_2 thin film	*E. coli* *Pseudomonas* *Bacillus sp* *Staphylococcus*	UV	100%	(Nithya et al., 2021)
Cu-doped TiO_2 thin film	*Phytophthorapalmivorahas*	UV	75% but concentrations >3% kill %100	(Natsir et al., 2021)
Ag- TiO_2 /PDMS thin film	*M.luteus* *S.maltophilia*	Visible irradiation	100%	(Chobba et al., 2021)
ZnO(wurtzite), TiO_2 , and ZnO- TiO_2 thin films	*A.flavusthan*	UV	100%	(Najibi Ilkhechi, Mozammel, & Yari Khosroushahi, 2021)

3. METHODS AND MATERIALS

3.1 Experimental Process

3.1.1 Production of Brookite Phase

The nanostructured TiO_2 sol was prepared using a mixture of titanium tetra isopropoxide (Ti [OCH(CH_3)2]4; (TTIP) Sigma-Aldrich), H2O, nitric acid (HNO_3), deionized water (DI), and isopropanol. First, titanium tetra isopropoxide (TTIP) was dissolved in isopropanol. Nitric acid was added dropwise in the solution under continuous stirring. Deionized water was added for hydrolysis. As a solution of TTIP:isopropanol:DI:AcAc a volume ratio of (0.4:4:0.1:0.2) was used. The solution was mixed using magnetic stirring for three hours at a room temperature of 22 ^oC.

3.1.2 Production of Anatase Phase

Titanium tetra isopropoxide (Ti $[OCH(CH_3)_2]_4$; (TTIP) Sigma-Aldrich) was mixed with acetic acid and ethanol with a molar ratio of 0.08:0.48:4, respectively. The mixture was stirred for two hours at a room temperature of 22 ^oC.

3.1.3 Production of Rutile Phase

Tetrabutyl orthotitanate (Ti $(OCH_2CH_2CH_2CH_3)_4$; TBOT) was dissolved in ethanol under vigorous stirring for 30 minutes. Then, in another beaker, ethanol was mixed with Hydrochloric acid (HCl) for 30 minutes. Afterward, the second solution in the other beaker was slowly added dropwise to the first solution under vigorous stirring until homogeneous. Then, preparation of the TiO_2 films with various crystal phases, the solutions prepared by the sol-gel process was spin-coated on the corning 2947 substrates. Next, the films were heat-treated at 450 ^oC for one hour, for brookite and anatase crystal phases, at 600 ^oC for the rutile crystal phase. After the heat treatment, one layer was formed on the surface of the films. Then, the films were coated with a spin coater again, paying attention to the TiO_2 solution coated side on the upper surface, and heat treatment and spin coating processes were continued until the films are 3-layered.

3.1.4 Production of ZnO (wurtzite)

The solution was prepared by dissolving zinc acetate dehydrate (ZnAc) in isopropanol. Dea (Diethanolamine), which is a surface-active material, is used to accelerate solving. Water was added for hydrolysis reactions, as a precursor solution of ZnAc:isopropanol:Dea: water, a volume ratio of 0.4:4:0.1:0.2 was used. The solution was mixed using magnetic stirring for one hour at 60°C.

3.1.5 Production of ZnO/TiO_2 material

The obtained solution in Section 3.1.4 was mixed with one of the leading TiO_2 solutions for brookite, rutile, or anatase phase at ZnO/TiO_2 volume ratios of 0, 0.01, 0.02, 0.05, 0.1, denoted as ZTA0-10, ZTB0-ZTB10, ZTR0-ZTR10, respectively. The final solutions were deposited on corning 2947 glass substrates by spin-coating deposition (1000 rpm/30 s), using a spin coater at room temperature (22^oC). After coating, ZnO films were immediately placed in a microprocessor-controlled (CWF 1100) furnace, heated at 450^oC. The films were taken out of the furnace and left at room temperature at the end of 1 hour. Finally, the all coatings and heat treatment processes were repeated two times in order to get 3-layered films.

3.1.6 Antibacterial measurements of thin films

Surfaces were needs to be smooth,1cm thick, and 5x5 cm^2 shapes. Six samples of a corning glass covered with thin films were prepared for the experiment; three samples to test bacteria and three to control groups. Each of these samples (TiO_2, ZnO/TiO_2) was analyzed by ISO 22196.

In antibacterial analysis, gram-positive "*Staphylococcus aureus*" and gram-negative "*Escherichia coli*" were used. The antibacterial activity of the films was evaluated by colony forming unit (CFU) counting. After incubation, the colonies were counted. CFU per ml was calculated for each sample at different time intervals (0-120 min) by using the following formula:

CFU/ml = No. of colonies × Dilution factor / volume inoculated

3.2 Characterizations

The absorbance spectra of composite films were measured using Labomed Spectro 22 UV–vis Spectrophotometer in the spectral range of 190–1100 nm wavelengths. The calculations of under the curve area, the entire width of half maximum of the absorbance data were performed by Origin 8.0 Software focusing the absorbance peak regions. The optical band gap energies of the composite films were calculated from the Tauc Plot since the thickness of the films was suitable for applying Beer-Lambert's Law. For identifying the films' crystal phases, an X-ray diffractometer (XRD, Philips PW-1800) with Cu-Kα radiation (The wavelength of Cu-Kα is 0.15406 nm) was used. The antibacterial response of the films was investigated using gram-positive "*Staphylococcus aureus*" (*S. aureus*) and gram-negative "*Escherichia coli*" (*E. coli*) according to the standard of ISO 22196. The initial dose of these bacteria's concentration was 10^5CFU/ml. Since TiO_2 shows antibacterial properties under UV light exposure and its photocatalytic effect is known, the antibacterial effect in the visible light region was investigated by doping with ZnO.

4. RESULTS AND DISCUSSION

4.1 XRD Results

The particle diameter size of different thin films was calculated according to Equation 2.7. The most crucial thing in the calculation is the theta value. Generally, theta value is found with two thetas and must need to convert single theta value to determine the diameter of particles properly. Then, the calculation and comparison of the XRD values were determined (Table 4.1 1).

Table 4.1.1. XRD values of different types of thin films and their diameter size

	Parameters		**Calculations**		
Thin films	**K**	**λ(A)**	**Peak positions 2θ**	**FWHM**	**D(nm)**
TiO_2 (anatase)	0.89	1.54	25.27	0.36	21.85
TiO_2 (brookite)	0.89	1.54	31.58	0.16	50.18

TiO_2 (rutile)	0.89	1.54	27.30	0.21	36.89
ZTA0(1st Peak)	0.89	1.54	25.27	0.36	21.85
ZTA0(2nd Peak)	0.89	1.54	37.69	0.34	24.19
ZTA1(1st Peak)	0.89	1.54	25.23	0.31	25.87
ZTA1(2nd Peak)	0.89	1.54	37.66	0.25	32.05
ZTA2 (1st Peak)	0.89	1.54	25.21	0.36	21.77
ZTA2 (2nd Peak)	0.89	1.54	37.67	0.25	32.12
ZTA5	0.89	1.54	25.19	0.43	18.66
ZTA10(1st Peak)	0.89	1.54	25.22	0.34	23.45
ZTA10(2nd Peak)	0.89	1.54	37.68	0.33	24.75
ZTA10(1st Peak	0.89	1.54	25.23	0.31	25.87
ZTA10(2nd Peak)	0.89	1.54	37.66	0.25	32.05
ZTA10(3rd Peak)	0.89	1.54	25.21	0.36	21.77
ZTA10(4th Peak)	0.89	1.54	37.67	0.25	32.12
ZTB0	0.89	1.54	31.58	0.16	50.18
ZTB1	0.89	1.54	31.54	0.35	23.07
ZTB2	0.89	1.54	31.55	0.34	23.97
ZTB5	0.89	1.54	31.60	0.48	16.98
ZTB10	0.89	1.54	31.76	0.59	13.61
ZTR0	0.89	1.54	27.30	0.21	36.89
ZTR1(1st Peak)	0.89	1.54	27.30	0.24	33.22
ZTR1(2nd Peak)	0.89	1.54	36.18	0.55	14.93
ZTR2(1st Peak)	0.89	1.54	27.30	0.21	36.96
ZTR2(2nd Peak)	0.89	1.54	36.08	0.25	32.86
ZTR5	0.89	1.54	27.30	0.21	37.21

ZTR10(1st peak)	0.89	1.54	36.08	0.28	29.49
ZTR10(2nd Peak)	0.89	1.54	25.76	5.58	1.44
ZTR10(3rd Peak)	0.89	1.54	31.59	0.92	8.85
ZTR10(4th Peak)	0.89	1.54	34.40	0.62	13.08
ZTR10(5th Peak)	0.89	1.54	36.19	0.64	12.73
ZnO(1st Peak)	0.89	1.54	31.75	0.15	52.87
ZnO((2nd Peak)	0.89	1.54	34.55	0.16	50.56
ZnO(3rd Peak)	0.89	1.54	36.44	0.16	51.11

In this study, decreased size diameter needs to be achieved after using ZnO as a dopant material. The average particle size of ZnO was found at 51.51 nanometers. The average size of pure TiO_2 phases anatase at 21.86 nm, brookite was at 50.18 nm, and rutile was at 36.9 nm. ZnO doped anatase TiO2 (ZTA) XRD data shows that a small concentration of ZnO doped increases the diameter size of TiO2 then decreases the composite size slowly after adding more ZnO concentration. In ZnO doped brookie TiO2(ZTB), XRD data shows that adding every amount of ZnO into brookite decreases the diameter size due to brookite orthomorphic structure. ZnO doped rutile TiO2 XRD data shows that the addition of ZnO also decreases the average particle size of pure slowly. This slow increase and decrease of particle size in ZTR(doped rutile) and ZTA(doped anatase) related to their tetragonal structure. Symmetrical structure affects the bond formation and hindering.

Figure 4.1.2. (a) shows that the films have a rare brookite phase, an orthorhombic crystal structure. A single crystallization peak (211) of the brookite phase at a 2θ value of 31.5° corresponds to ICDD Card No. 04-019-9878. In Figure 4.1.1.(c), the sharp diffraction peaks at 25.2°, 37.7°, and 47.8° theta values are indexed to the (101), (004), and (200). Planes of the anatase phase of TiO2 correspond to 21-1272 according to ICDD Card. In Figure 4.1.1. (d), the peaks at the 2θ values of 27.31°, 36.12°, and 41.25° are fitted well with the (110), (101), and (111) planes of the rutile phase of TiO_2 (ICDD Card No. 21-1276), respectively. These (anatase and rutile) are tetragonal phases of TiO_2.

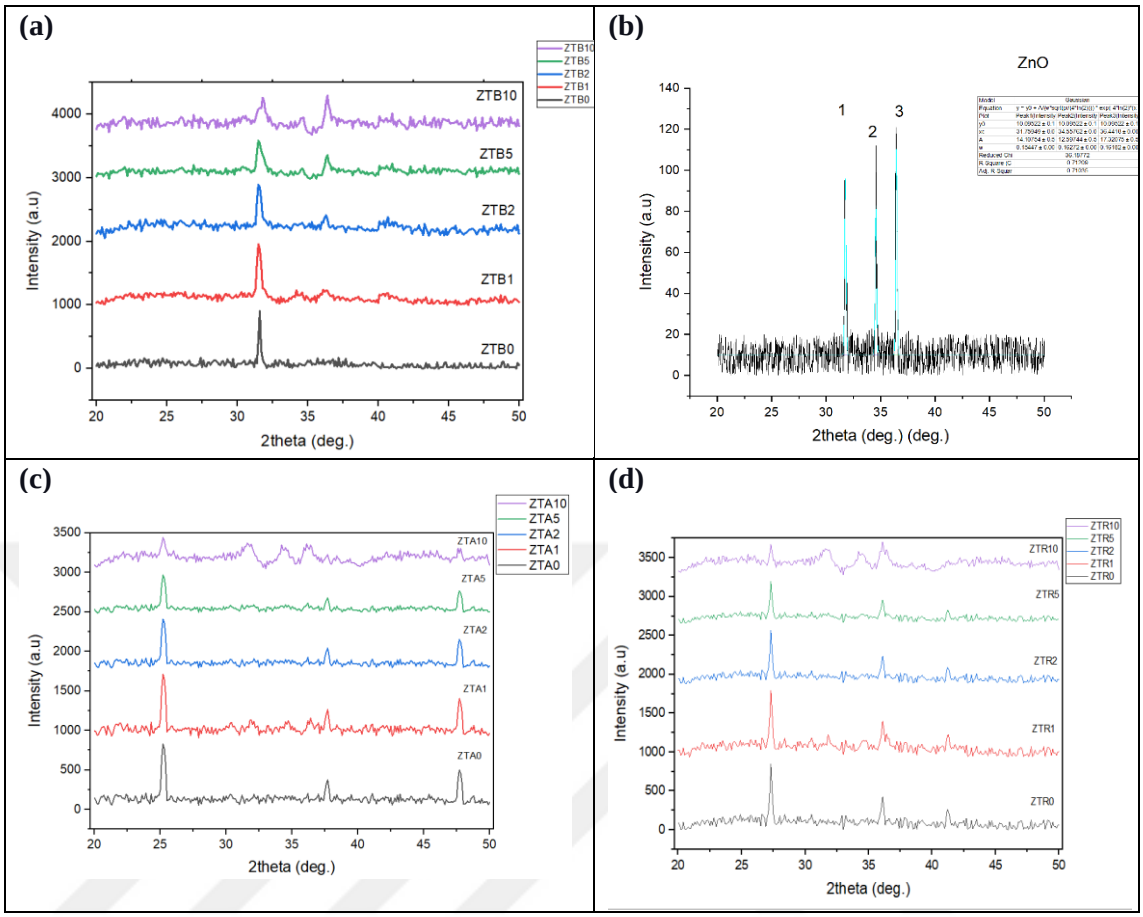

Figure 4.1.3. XRD response of **(a)** ZnO doped TiO_2 brookite films with various ZnO/TiO_2 doping ratios, **(b)** ZnO film and parameter calculations, **(c)** ZnO doped TiO_2 anatase films with various ZnO/TiO_2 doping ratios, **(d)** ZnO doped TiO_2 rutile films with various ZnO/TiO_2 doping ratios.

4.2 Optical Results

Absorption spectra of pure TiO_2 films and ZnO doped TiO_2 films were analyzed using UV-vis spectrophotometers, as shown in Figure 4.2.1. High absorbance values are seen between at 200-500 range. According to absorbance-wavelength graphs, the addition of ZnO can enhance the absorbance rate of all three phases. The high absorbance value of ZnO can decrease the absorbance range of Pure TiO_2 phases because of dilution of pure TiO_2 absorbance ability reduce, and the addition of ZnO introduces its photon absorbance rate. Recombination of rate increases, and absorption of doped nanocomposites decreases. The addition of ZnO also affects the resonance ratio and homogeneity of the material. Doped material may enhance the photocatalytic activity, but the optimum

amount of dopant addition so important for homogeneity concerns. A comparison of different volumes of ZnO doped anatase, brookite, and rutile was determined (Figure 4.2.1 to 4.2.4). In normal conditions, the homogeneity of material is determined by the relation between resonance ratio and normalized width. When the resonance ratio increase and normalize width decreases, that implies composites reach a more homogenous structure. According to calculations, the addition of ZnO dopant decreases the resonance ratio and increases the normalized width, which is vice versa of literature information. However, our studies do not ultimately increase or decrease; it has some ranges in which composites resonance ratio increases with ZnO. This result provides a piece of good information such as critical point to cut down dopant addition to getting the more homogenous structure. Further studies can arrange their dopant addition to these ranges to get more homogenous material. ZTA5-10, ZTB5-10, and ZTR5-10 concentration ranges are critical for the homogeneity shift for excessive dopant addition (Table 4.2.1).

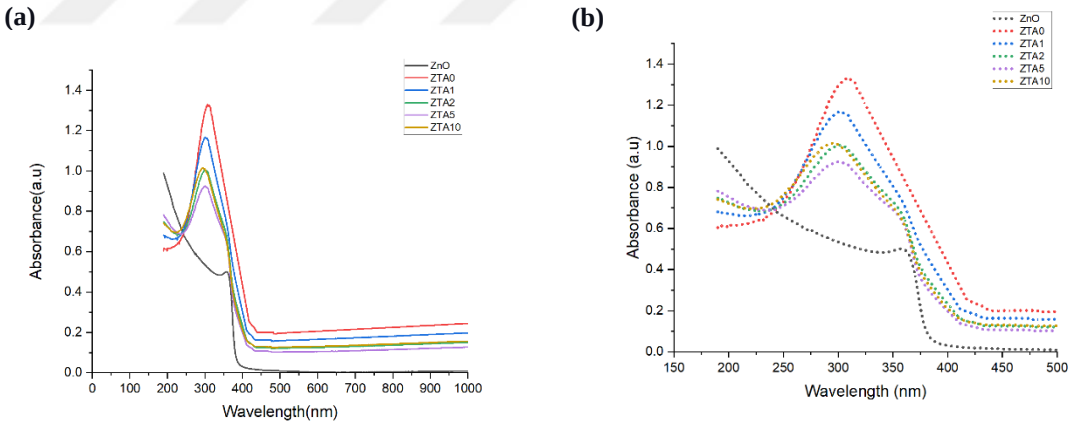

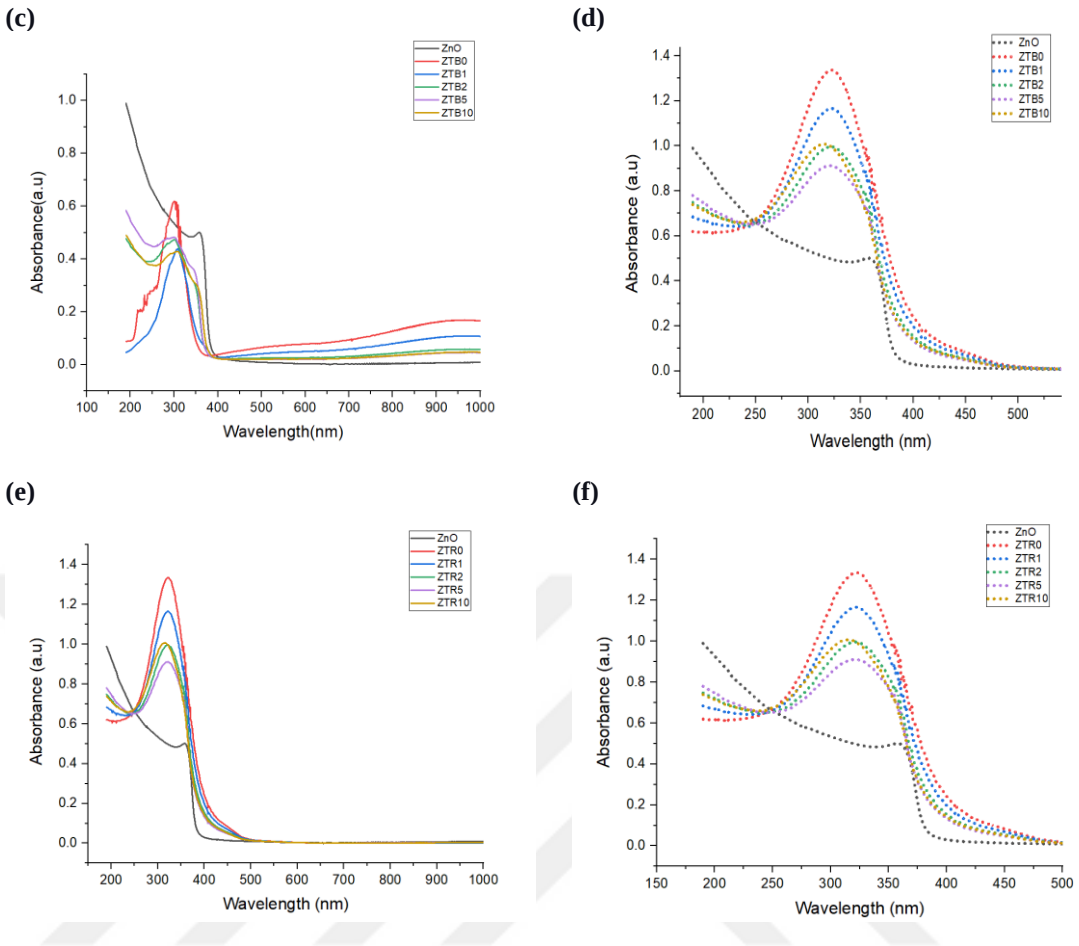

Figure 4.2.1. Absorbance wavelength spectrum of ZnO and ZnO doped TiO_2. In **(a-c-e)** graphs show the range between 200-1000 spectrum, and **(b-d-f)** graphs show the detailed range between 200-500 range spectrum.

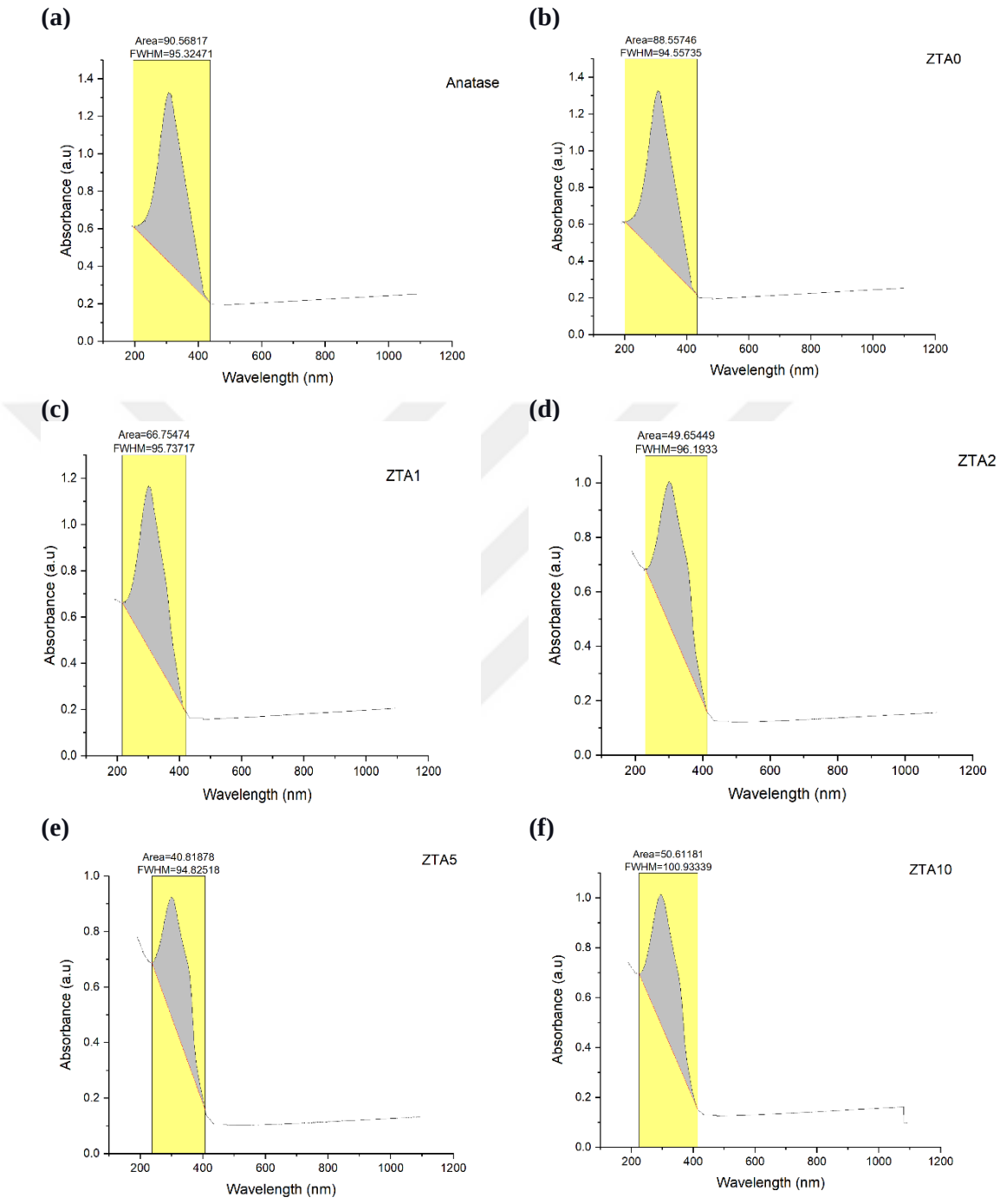

Figure 4.2.2. Resonant band representation of pure **(a)** and ZnO doped **(b-f)** anatase TiO_2

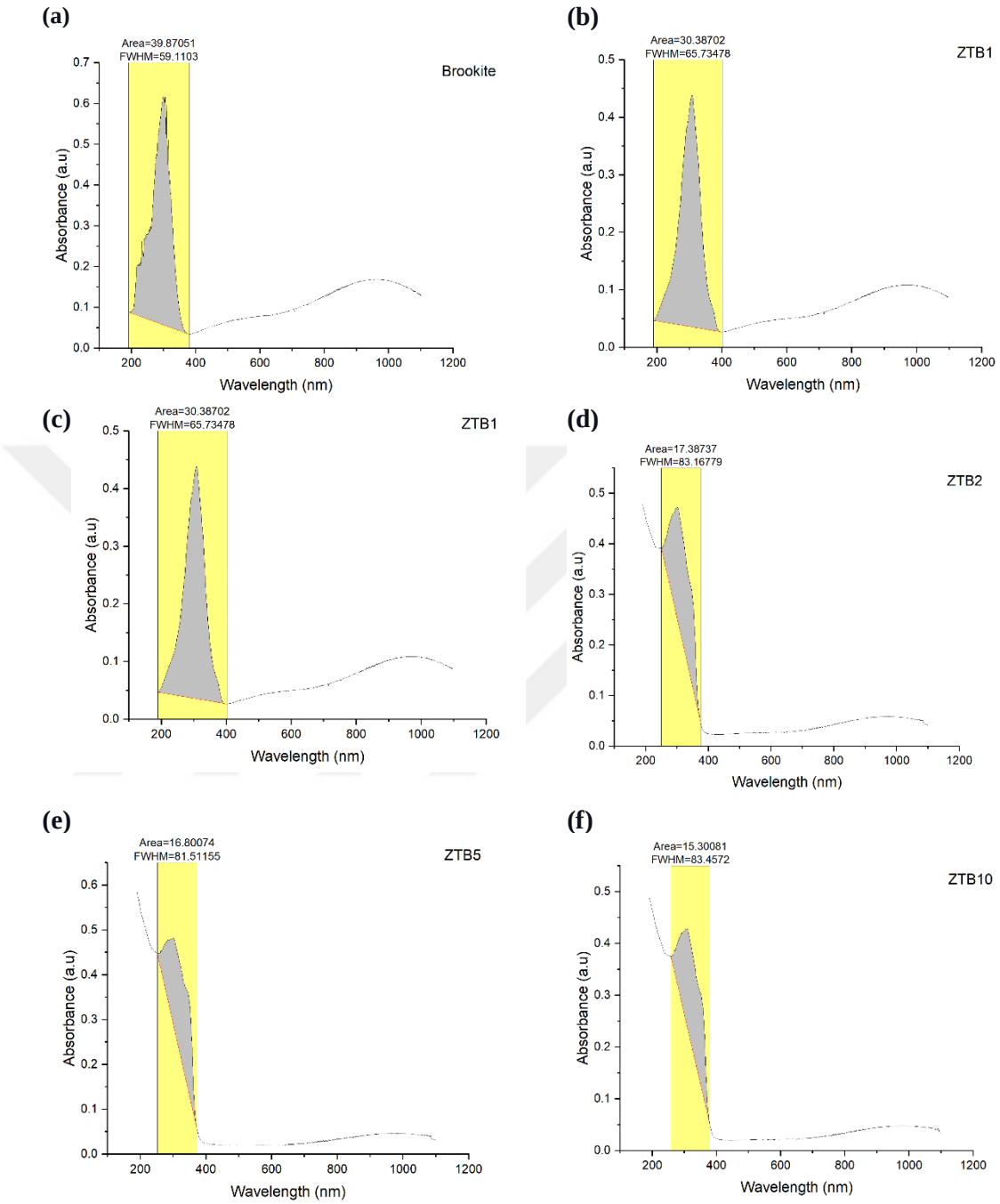

Figure 4.2.3. Resonant band representation of pure **(a)** and ZnO doped **(b-f)** brookite TiO_2

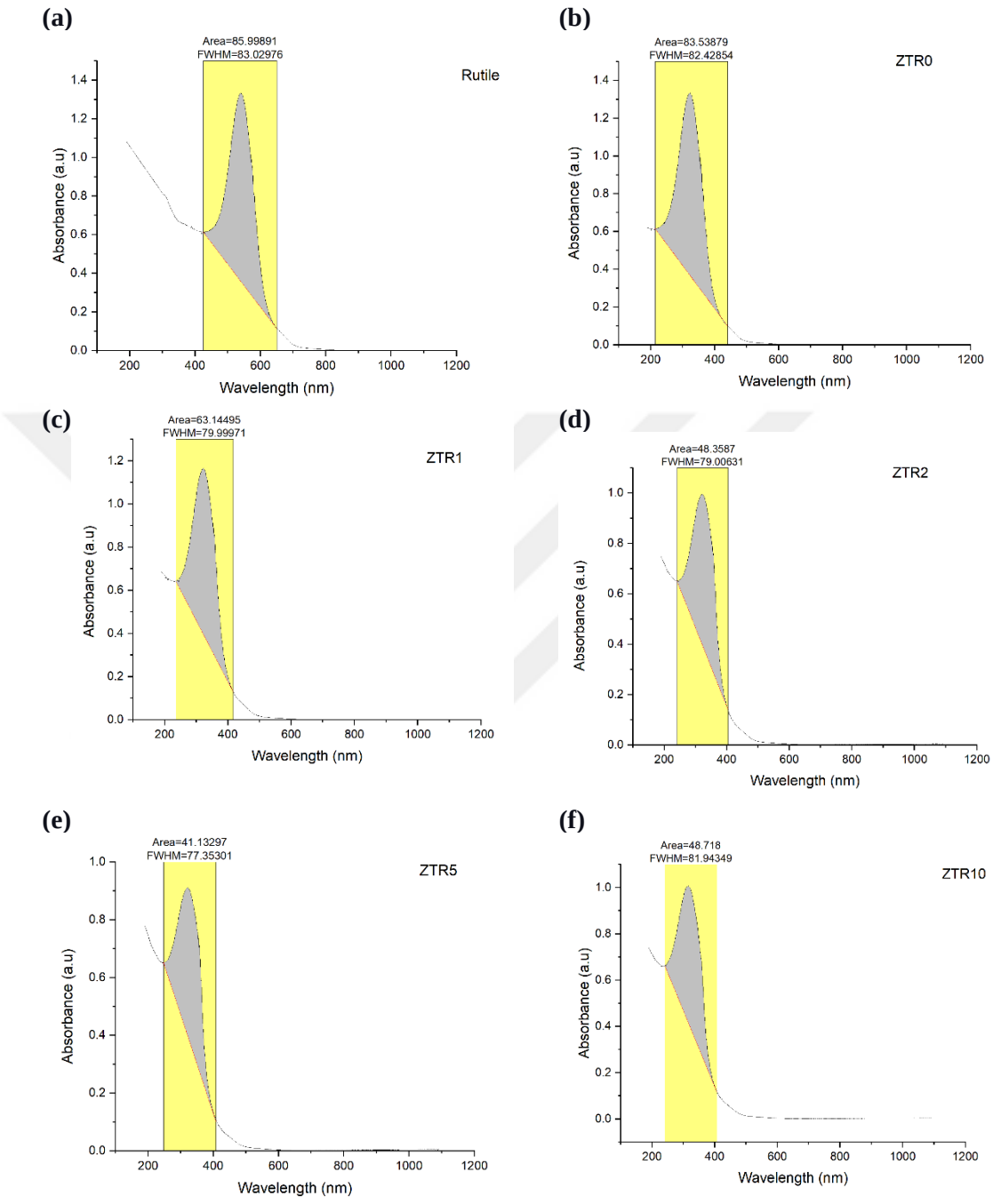

Figure 4.2.4. Resonant bands representation of pure **(a)** and ZnO doped **(b-f)** rutile TiO_2.

Table 4.2.1. Calculation of resonance ratio and normalized width of pure and ZnO doped TiO_2

Thin films	Area of resonant band	Area of non-resonant background	Resonance ratio	Width of resonant band	Height of resonant band	Normalized width
Pure TiO_2 (anatase)	90.56	100.52	0.90	95.32	0.90	104.97
Pure TiO_2 (brookite)	39.87	11.46	3.47	59.11	0.56	105.15
Pure TiO_2 (rutile)	85.99	87.29	0.98	83.02	0.98	84.11
ZTA0	88.55	97.13	0.91	94.55	0.89	105.14
ZTA1	66.75	87.41	0.76	95.73	0.70	135.66
ZTA2	49.65	77.41	0.64	96.19	0.53	180.24
ZTA5	40.81	72.15	0.56	94.82	0.44	212.55
ZTA10	50.61	80.79	0.62	100.93	0.52	191.56
ZTB0	39.90	11.34	3.51	59.13	0.56	105.20
ZTB1	30.38	7.75	3.91	65.73	0.40	163.06
ZTB2	17.38	27.52	0.63	83.16	0.22	364.62
ZTB5	16.80	30.29	0.55	81.51	0.21	378.41
ZTB10	15.30	35.76	0.42	83.45	0.19	431.66
ZTR0	83.53	81.09	1.03	82.42	0.96	85.17
ZTR1	63.14	70.08	0.90	79.99	0.77	103.60
ZTR2	48.35	64.85	0.74	79.00	0.60	130.06
ZTR5	41.13	60.50	0.67	77.35	0.52	146.87
ZTR10	48.71	64.83	0.75	81.94	0.60	136.11

4.3 Bandgap Energy

In band energy analysis, the Tauc pilot was used to measure materials' band-gap energies (Equation 4.3.1). In general, Titanium dioxide (TiO_2) is an excellent semiconductor in terms of bandgap energy, such as anatase 3.20 eV, rutile 3.00 eV, and brookite 3.13 eV (Linsebigler, Lu, & Yates, 1995; Thiyagarajan, Sivakumar, & Rajangam, 2016; Wang, He, Lai, & Fan, 2014). In this part, the photocatalytic ability of pure TiO_2 and ZnO doped TiO_2 was determined. In a normal condition, ZnO addition needs to increase the bandgap energy of pure TiO_2, but TiO_2 is an indirect semiconductor, and ZnO is a direct conductor. Thus every possible indirect and direct graphs need to be evaluated for optimum results (Figure 4.3.1). These graphs find from the absorbance value of every single material. In direct conduction, the r variable equal to 2 and the indirect conduction r variable equal to ½. After creating their Tauc plots, ZnO doped anatase tend to direct conductor, ZnO doped brookite tend to the indirect conductor, and ZnO doped rutile tend to act like a direct conductor. Discrimination of indirect and direct conduction is done by using the Tauc plot. ZnO normal bandgap energy around at 3.37 eV (Firdaus, Rizam, Rusop, & Hidayah, 2012). The addition of ZnO dopant needs to increase the original bandgap energy of pure TiO_2 phases. Due to this reason, (a),(d),(e) in Figure 4.3.1 shows that the addition of ZnO dopant increases the original band gap energy of TiO_2.

$$(\alpha h\nu) = B(h\nu - E_g)^r \qquad (4.3.1)$$

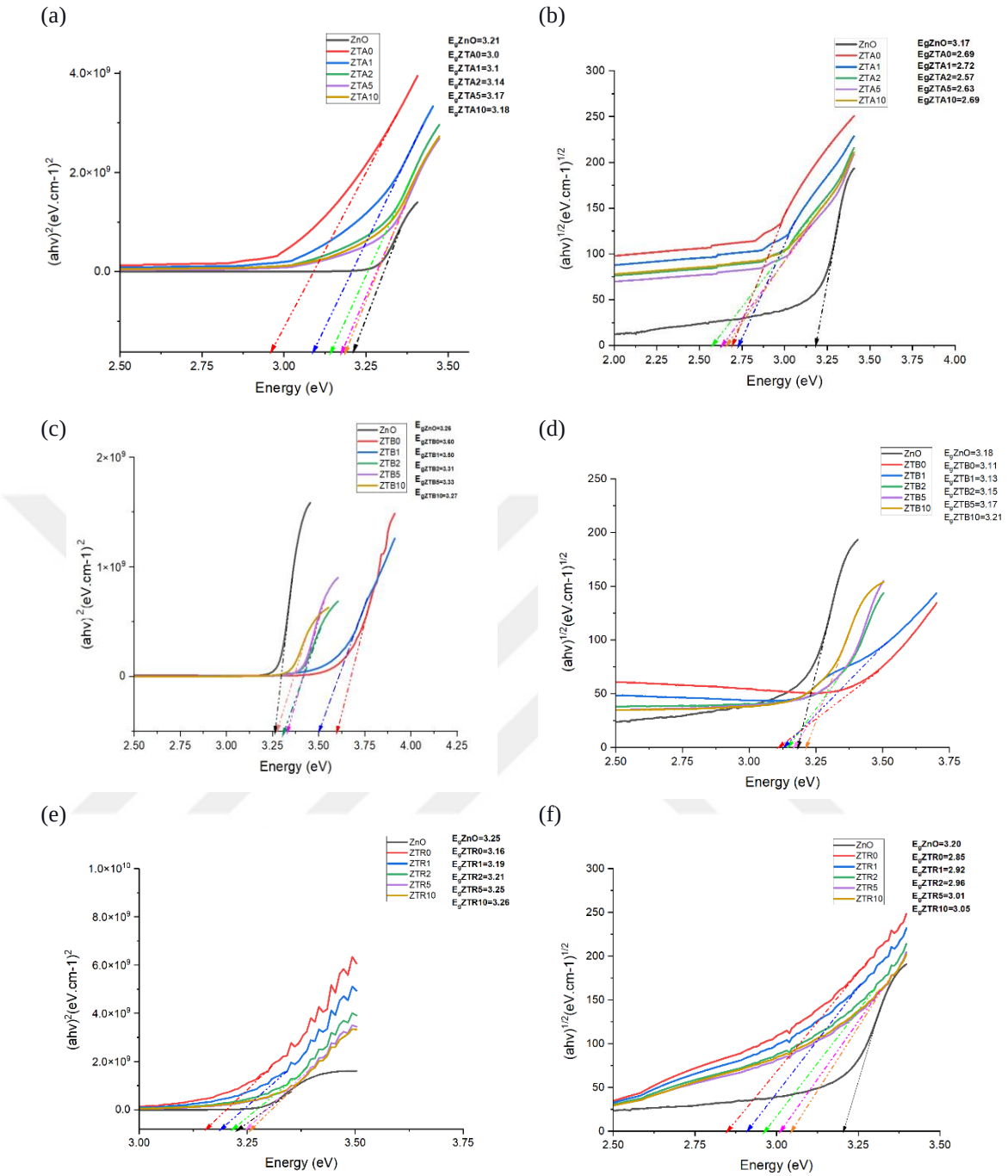

Figure 4.3.2. Tauc Plot of pure ZnO and ZnO doped Anatase, Brookite, and Rutile phases of TiO_2 with various ZnO/TiO_2 ratios. The extrapolation of the curves shows the optical energy band gap of ZTA, ZTR, and ZTB.

Table 4.3.1. Bandgap energy values of different types of doped material derived from the Tauc plot.

Film type	Direct(eV)	Indirect(eV)
ZnO	3.21	3.17
ZTA0	3.0	2.69
ZTA1	3.1	2.72
ZTA2	3.14	2.57
ZTA5	3.17	2.63
ZTA10	3.18	2.69
ZTB0	3.60	3.11
ZTB1	3.50	3.13
ZTB2	3.31	3.15
ZTB5	3.33	3.17
ZTB10	3.27	3.21
ZTR0	3.16	2.85
ZTR1	3.19	2.92
ZTR2	3.21	2.96
ZTR5	3.25	3.01
ZTR10	3.26	3.05

4.4 Antibacterial Activity

Figure 4.4.1 presents the antibacterial response of films with respect to the time for *E. coli* and *S.aureus*. *E. coli* count reduced from 10^5 to 10^4 with 120 min of irradiation time for pure brookite TiO_2 film. A dramatic decrease of the bacteria number for both bacteria was observed for ZnO/TiO_2 composite films compared with that of TiO_2 films under the lighting with visible light. After 120 min. of light exposure, the bactericidal survival decrease of ZTA0, ZTA1, ZTA2, ZTA5, and ZTA10 films against E. coli were 10^0, $3x10^1$, 10^2, $2x10^2$ and $7x10^3$, respectively. Meanwhile, exhibiting a similar trend, the bactericidal survival decrease of ZTA0, ZTA1, ZTA2, ZTA5, and ZTA10 films against S. aureus were 10^0, $5x10^1$, $2x10^2$, $6x10^3$ and 10^4, respectively. For ZTB2-ZTB10 films, complete inactivation of the *E. coli* was recorded at 120, 90, and 75 min of light exposure, respectively. Since TiO_2 shows antibacterial properties under UV light exposure and its photocatalytic effect is known, the antibacterial effect in the visible light region was investigated by doping with ZnO. These results show that the content of ZnO in the ZnO/TiO_2 composite films plays a significant role for enhancing the antibacterial activity of the films in the absence of UV light.

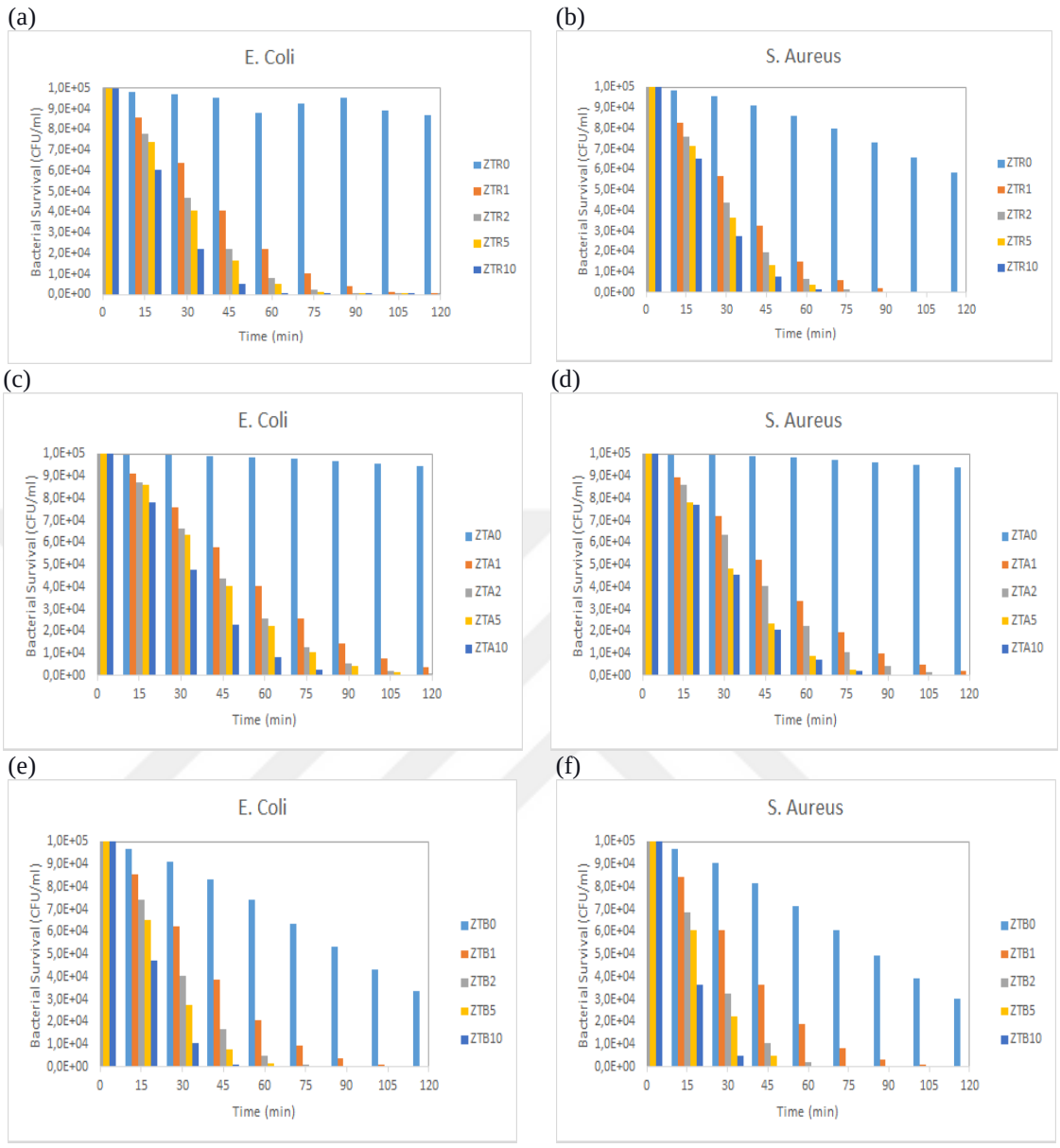

Figure 4.4.3. Antibacterial response of ZnO doped Anatase, Brookite, and Rutile phases of TiO_2 with various ZnO/TiO_2 ratios under light exposure for *E. Coli* and *S. Aureus*.

5. CONCLUSION

In conclusion, XRD results show that the particle size of TiO_2 can be reduced in the brookite phase rather than anatase and rutile due to brookite's large volume. However, anatase and rutile also show remarkable diameter size drop when the concentration is appropriately arranged. Due to their stability traits, anatase and rutile particle size decrease slowly. UV data show that the resonance ratio is essential for cell homogeneity and dispersibility. Due to this reason addition of dopant materials needs to be controlled by stoichiometry for optimum homogeneity. Using the sol-gel method provides the minor homogeneity range for ZnO doped TiO_2 in a concentration of doped ZTA5-10, ZTB5-10, and ZTR5-10. After all these properties, band gap energy enhancement of ZnO was showed by uısing Tauc plot. Direct ZnO doped anatase TiO_2, direct ZnO doped rutile and indirect ZnO doped brookite conduction bands showed. Accoring to antibacterial activity test results, the ZnO doping of composite films boost the inactivation of bacteria under visible light. This thesis mainly focused on discovering how dopant material can enhance the activity of pure material and how these enhanced traits can be used on optical and antibacterial activity. Therefore, ZnO/TiO_2 composite films can give an alternative solution for antibacterial surface applications under visible light.

REFERENCES

Aguilar, G. (2018). Introductory Chapter: A Brief Semblance of the Sol-Gel Method in Research. In.

Ambigadevi, J., Senthil Kumar, P., Vo, D.-V. N., Hari Haran, S., & Srinivasa Raghavan, T. N. (2021). Recent developments in photocatalytic remediation of textile effluent using semiconductor based nanostructured catalyst: A review. *Journal of Environmental Chemical Engineering, 9*(1). doi:10.1016/j.jece.2020.104881

Arce-Sarria, A., Machuca-Martínez, F., Bustillo-Lecompte, C., Hernández-Ramírez, A., & Colina-Márquez, J. (2018). Degradation and Loss of Antibacterial Activity of Commercial Amoxicillin with TiO2/WO3-Assisted Solar Photocatalysis. *Catalysts, 8*(6). doi:10.3390/catal8060222

Bensouici, F., Souier, T., Dakhel, A. A., Iratni, A., Tala-Ighil, R., & Bououdina, M. (2015). Synthesis, characterization and photocatalytic behavior of Ag doped TiO2 thin film. *Superlattices and Microstructures, 85*, 255-265. doi:10.1016/j.spmi.2015.05.028

Brady, J. B., & Boardman, S. J. (1995). Introducing Mineralogy Students to X-Ray Diffraction through Optical Diffraction Experiments using Lasers. *Journal of Geological Education, 43*(5), 471-476. doi:10.5408/0022-1368-43.5.471

C. Brinker, G. S. (1990). *The Physics and Chemistry of Sol-Gel Processing* (1st ed.). Academic Press: Academic Press.

Chobba, M. B., Weththimuni, M. L., Messaoud, M., Urzi, C., Bouaziz, J., De Leo, F., & Licchelli, M. (2021). Ag-TiO2/PDMS nanocomposite protective coatings: Synthesis, characterization, and use as a self-cleaning and antimicrobial agent. *Progress in Organic Coatings, 158*, 106342. doi:https://doi.org/10.1016/j.porgcoat.2021.106342

Deák, Á., Janovák, L., Csapó, E., Ungor, D., Palinko, I., Puskás, S., . . . Dekany, I. (2016). Layered double oxide (LDO) particle containing photoreactive hybrid layers with tunable superhydrophobic and photocatalytic properties. *Applied Surface Science, 389*. doi:10.1016/j.apsusc.2016.07.127

Dulian, P., Nachit, W., Jaglarz, J., Zięba, P., Kanak, J., & Żukowski, W. (2019). Photocatalytic methylene blue degradation on multilayer transparent TiO2 coatings. *Optical Materials, 90*, 264-272. doi:10.1016/j.optmat.2019.02.041

Farzaneh, A., Mohammadzadeh, A., Esrafili, M. D., & Mermer, O. (2019). Experimental and theoretical study of TiO2 based nanostructured semiconducting

humidity sensor. *Ceramics International, 45*(7), 8362-8369. doi:10.1016/j.ceramint.2019.01.144

Firdaus, C. M., Rizam, M. S. B. S., Rusop, M., & Hidayah, S. R. (2012). Characterization of ZnO and ZnO: TiO2 Thin Films Prepared by Sol-Gel Spray-Spin Coating Technique. *Procedia Engineering, 41*, 1367-1373. doi:10.1016/j.proeng.2012.07.323

Freire, T., Fragoso, A. R., Matias, M., Vaz Pinto, J., Marques, A. C., Pimentel, A., . . . Nunes, D. (2021). Enhanced solar photocatalysis of TiO2 nanoparticles and nanostructured thin films grown on paper. *Nano Express*. doi:10.1088/2632-959X/abed40

Ghouri, Z. K., Elsaid, K., Abdala, A., Al-Meer, S., & Barakat, N. A. M. (2018). Surfactant/organic solvent free single-step engineering of hybrid graphene-Pt/TiO2 nanostructure: Efficient photocatalytic system for the treatment of wastewater coming from textile industries. *Sci Rep, 8*(1), 14656. doi:10.1038/s41598-018-33108-4

Gospodonova, D., Ivanova, I., & Vladkova, T. (2021). Fabrication and Characterization of Antimicrobial Magnetron Cosputtered TiO2/Ag/Cu Composite Coatings. *Coatings, 11*(4). doi:10.3390/coatings11040473

I M Joni, L. N. a. C. P. (2018). Characteristics of TiO2 particles prepared by simple solution method
using TiCl3 precursor. *Journal of Physics: Conf. Series*. doi:0.1088/1742-6596/1080/1/012042

Jilani, A., Abdel-wahab, M. S., & Hammad, A. H. (2017). Advance Deposition Techniques for Thin Film and Coating. In *Modern Technologies for Creating the Thin-film Systems and Coatings*.

Khlyustova, A., Sirotkin, N., Kusova, T., Kraev, A., Titov, V., & Agafonov, A. (2020). Doped TiO2: the effect of doping elements on photocatalytic activity. *Materials Advances, 1*(5), 1193-1201. doi:10.1039/d0ma00171f

Kolathupalayam Shanmugam, B., Rangaraj, S., Subramani, K., Srinivasan, S., Aicher, W. K., & Venkatachalam, R. (2020). Biomimetic TiO2-chitosan/sodium alginate blended nanocomposite scaffolds for tissue engineering applications. *Mater Sci Eng C Mater Biol Appl, 110*, 110710. doi:10.1016/j.msec.2020.110710

Kumar, R. S., Ryu, J., Kim, H., Mergu, N., Park, J.-Y., Shin, H.-J., . . . Son, Y.-A. (2021). Synthesis, characterization, and photocatalytic disinfection studies of porphyrin dimer/TiO2-based photocatalyst. *Journal of Molecular Structure, 1236*. doi:10.1016/j.molstruc.2021.130276

Lamouchi, W., Slama, S. B., Saadallah, F., & Bouaicha, M. (2021). Nickel doping induced amorphization of brookite TiO2: Photoluminescence enhancement. *Optik, 227*. doi:10.1016/j.ijleo.2020.166123

Li, H., Cui, Q., Feng, B., Wang, J., Lu, X., & Weng, J. (2013). Antibacterial activity of TiO2 nanotubes: Influence of crystal phase, morphology and Ag deposition. *Applied Surface Science, 284*, 179-183. doi:10.1016/j.apsusc.2013.07.076

Lin, X., Sun, M., Gao, B., Ding, W., Zhang, Z., Anandan, S., & Umar, A. (2021). Hydrothermally regulating phase composition of TiO2 nanocrystals toward high photocatalytic activity. *Journal of Alloys and Compounds, 850*. doi:10.1016/j.jallcom.2020.156653

Linsebigler, A. L., Lu, G., & Yates, J. T. (1995). Photocatalysis on TiO2 Surfaces: Principles, Mechanisms, and Selected Results. *Chemical Reviews, 95*(3), 735-758. doi:10.1021/cr00035a013

Luttrell, T., Halpegamage, S., Tao, J., Kramer, A., Sutter, E., & Batzill, M. (2014). Why is anatase a better photocatalyst than rutile?--Model studies on epitaxial TiO2 films. *Sci Rep, 4*, 4043. doi:10.1038/srep04043

Mardare, D., Iacomi, F., Cornei, N., Girtan, M., & Luca, D. (2010). Undoped and Cr-doped TiO(2) thin films obtained by spray pyrolysis. *Thin Solid Films, 518*, 4586-4589. doi:10.1016/j.tsf.2009.12.037

Medvids, A., Onufrijevs, P., Kaupužs, J., Eglitis, R., Padgurskas, J., Zunda, A., . . . Varnagiris, S. (2021). Anatase or rutile TiO2 nanolayer formation on Ti substrates by laser radiation: Mechanical, photocatalytic and antibacterial properties. *Optics & Laser Technology, 138*. doi:10.1016/j.optlastec.2020.106898

Mérai, L., Deák, Á., Sebok, D., Csapó, E., Kolumban, T., Hopp, B., . . . Janovák, L. (2018). Photoreactive composite coating with composition dependent wetting properties. *Express Polymer Letters, 12*, 1061-1071. doi:10.3144/expresspolymlett.2018.93

Mutuma, B. K., Shao, G. N., Kim, W. D., & Kim, H. T. (2015). Sol-gel synthesis of mesoporous anatase-brookite and anatase-brookite-rutile TiO2 nanoparticles and their photocatalytic properties. *J Colloid Interface Sci, 442*, 1-7. doi:10.1016/j.jcis.2014.11.060

Najibi Ilkhechi, N., Mozammel, M., & Yari Khosroushahi, A. (2021). Antifungal effects of ZnO, TiO2 and ZnO-TiO2 nanostructures on Aspergillus flavus. *Pesticide Biochemistry and Physiology, 176*, 104869. doi:https://doi.org/10.1016/j.pestbp.2021.104869

Natsir, M., Maulidiyah, M., Watoni, A. H., Arif, J., Sari, A., Salim, L. O. A., . . . Nurdin, M. (2021). Synthesis and charcterization of Cu-doped TiO2 (Cu/TiO2) nanoparticle as antifungal phytophthora palmivora. *Journal of Physics: Conference Series, 1899*(1), 012039. doi:10.1088/1742-6596/1899/1/012039

Nithya, N., Kumar, E. R., Magesh, G., Arun, A. P., Abou-Melha, K. S., Badr, G., . . . Rahale, C. S. (2021). Evaluation of gas sensor behaviour of Sm3+ doped TiO2 nanoparticles. *Journal of Materials Science: Materials in Electronics*. doi:10.1007/s10854-021-06246-1

Norton, D. P., Heo, Y. W., Ivill, M. P., Ip, K., Pearton, S. J., Chisholm, M. F., & Steiner, T. (2004). ZnO: growth, doping & processing. *Materials Today, 7*(6), 34-40. doi:https://doi.org/10.1016/S1369-7021(04)00287-1

Ojha, A., & Thareja, P. (2020). Graphene-based nanostructures for enhanced photocatalytic degradation of industrial dyes. *Emergent Materials, 3*(2), 169-180. doi:10.1007/s42247-020-00081-6

Pant, Park, & Park. (2019). Recent Advances in TiO2 Films Prepared by Sol-gel Methods for Photocatalytic Degradation of Organic Pollutants and Antibacterial Activities. *Coatings, 9*(10). doi:10.3390/coatings9100613

Pantaroto, H. N., Ricomini-Filho, A. P., Bertolini, M. M., Dias da Silva, J. H., Azevedo Neto, N. F., Sukotjo, C., . . . Barao, V. A. R. (2018). Antibacterial photocatalytic activity of different crystalline TiO2 phases in oral multispecies biofilm. *Dent Mater, 34*(7), e182-e195. doi:10.1016/j.dental.2018.03.011

Patil, M., Shaikh, S., & Ibram, G. (2015). Recent Advances on TiO2 Thin Film Based Photocatalytic Applications (A Review). *Current Nanoscience, 11*. doi:10.2174/1573413711666150212235054

Phuinthiang, P., Trinh, D. T. T., Channei, D., Ratananikom, K., Sirilak, S., Khanitchaidecha, W., & Nakaruk, A. (2021). Novel Strategy for the Development of Antibacterial TiO2 Thin Film onto Polymer Substrate at Room Temperature. *Nanomaterials, 11*(6). doi:10.3390/nano11061493

Pleskova, S. N., Golubeva, I. S., Verevkin, Y. K., Pershin, E. A., Burenina, V. N., & Korolichin, V. V. (2011). Photoinduced bactericidal activity of TiO2 films. *Applied Biochemistry and Microbiology, 47*(1), 23-26. doi:10.1134/S0003683811010091

Qureshi, A. A., Javed, S., Javed, H. M. A., Akram, A., Mustafa, M. S., Ali, U., & Nisar, M. Z. (2021). Facile formation of SnO2–TiO2 based photoanode and Fe3O4@rGO based counter electrode for efficient dye-sensitized solar cells.

Materials Science in Semiconductor Processing, 123. doi:10.1016/j.mssp.2020.105545

Rajendhiran, R., Deivasigamani, V., Palanisamy, J., Pitchaiya, S., Eswaramoorthy, N., & Masan, S. (2021). Plectranthus amboinicus Leaf Extract Synthesized Spherical like-TiO2 Photoanode for Dye-Sensitized Solar Cell Application. *Silicon*. doi:10.1007/s12633-020-00709-6

Sabri, Y. M., Kandjani, A. E., Rashid, S. S. A. A. H., Harrison, C. J., Ippolito, S. J., & Bhargava, S. K. (2018). Soot template TiO2 fractals as a photoactive gas sensor for acetone detection. *Sensors and Actuators B: Chemical, 275*, 215-222. doi:10.1016/j.snb.2018.08.059

Sayılkan, F., Asiltürk, M., Kiraz, N., Burunkaya, E., Arpaç, E., & Sayılkan, H. (2009). Photocatalytic antibacterial performance of Sn4+-doped TiO2 thin films on glass substrate. *Journal of Hazardous Materials, 162*(2), 1309-1316. doi:https://doi.org/10.1016/j.jhazmat.2008.06.043

Sivakumar, A., Kalaiarasi, S., Dhas, S. S. J., Almansour, A. I., Kumar, R. S., Arumugam, N., & Dhas, S. A. M. B. (2021). Assessment of shock wave resistance on brookite TiO2. *Journal of Materials Science: Materials in Electronics*. doi:10.1007/s10854-021-06063-6

Skoog, D. A., West, D. M., Holler, F. J., & Crouch, S. R. (2004). *Fundamentals of Analytical Chemistry*: Thomson-Brooks/Cole.

Su, X., He, Q., Yang, Y.-e., Cheng, G., Dang, D., & Yu, L. (2021). Free-standing nitrogen-doped TiO2 nanorod arrays with enhanced capacitive capability for supercapacitors. *Diamond and Related Materials, 114*. doi:10.1016/j.diamond.2020.108168

Tan, Y., & Resasco, D. E. (2005). Dispersion of Single-Walled Carbon Nanotubes of Narrow Diameter Distribution. *The Journal of Physical Chemistry B, 109*(30), 14454-14460. doi:10.1021/jp052217r

Thiyagarajan, D., Sivakumar, R., & Rajangam, I. (2016). Growth of micro flower rutile TiO2 films by chemical bath deposition technique: Study on the properties of structural, surface morphological, vibrational, optical and compositional. *Surfaces and Interfaces, 4*. doi:10.1016/j.surfin.2016.09.006

Valerio, A., & Morelhão, S. (2019). *Usage of Scherrer's formula in X-ray diffraction analysis of size distribution in systems of monocrystalline nanoparticles*.

Varshney, G., Kanel, S. R., Kempisty, D. M., Varshney, V., Agrawal, A., Sahle-Demessie, E., . . . Nadagouda, M. N. (2016). Nanoscale TiO2 films and their

application in remediation of organic pollutants. *Coordination Chemistry Reviews, 306*, 43-64. doi:https://doi.org/10.1016/j.ccr.2015.06.011

Wang, Y., He, Y., Lai, Q., & Fan, M. (2014). Review of the progress in preparing nano TiO2: an important environmental engineering material. *J Environ Sci (China), 26*(11), 2139-2177. doi:10.1016/j.jes.2014.09.023

Yemmireddy, V. K., & Hung, Y. C. (2017). Using Photocatalyst Metal Oxides as Antimicrobial Surface Coatings to Ensure Food Safety-Opportunities and Challenges. *Compr Rev Food Sci Food Saf, 16*(4), 617-631. doi:10.1111/1541-4337.12267

Yu, J., Li, L., Qian, Y., Lou, H., Yang, D., & Qiu, X. (2018). Facile and Green Preparation of High UV-Blocking Lignin/Titanium Dioxide Nanocomposites for Developing Natural Sunscreens. *Industrial & Engineering Chemistry Research, 57*(46), 15740-15748. doi:10.1021/acs.iecr.8b04101

Zainab, N. J., Olfat, A. M., & Faisal, L. A. (2019). Studying the effect of synthesized Nano-Titanium Dioxide via two phases on the pseudomonas aeruginosa and portus bacteria as antimicrobial agents.

Zhang, H., & Banfield, J. F. (2014). Structural characteristics and mechanical and thermodynamic properties of nanocrystalline TiO2. *Chem Rev, 114*(19), 9613-9644. doi:10.1021/cr500072j

ÖZGEÇMİŞ

Kişisel Bilgiler
Adı Soyadı : Mehmet Eymen Sümer

Eğitim Durumu
Lisans Öğrenimi : Sabancı Üniversitesi
Yüksek Lisans Öğrenimi : Kadir Has Universitesi
Bildiği Yabancı Diller : İngilizce

İş Deneyimi
Çalıştığı Kurumlar ve Tarihleri: